UNIVERSITÀ DEGLI STUDI DI MESSINA

DIPARTIMENTO DI SCIENZE CHIMICHE, BIOLOGICHE, FARMACEUTICHE ED AMBIENTALI

Dottorato Di Ricerca in "Biologia Applicata e Medicina Sperimentale
Coordinatrice Prof.ssa Emanuela Esposito
Settore Scientifico Disciplinare: BIOS-15/A - Microbiologia

MID-TERM EVALUATION OF THE ANTIFOULING PROPERTIES OF IONIC LIQUIDS BASED COATINGS APPLIED ON LIMESTONE AND MARBLE PROBES IN MARINE ENVIRONMENT

Dottoranda
Marika Luci
Firmato digitalmente da Marika Luci
Data: 2025.07.01 13:03:38 +02'00'
Dott.ssa Marika Luci

Tutor
Firmato digitalmente da Clara Enza Urzi'
Data: 30.06.2025 16:00:08 CEST
Organizzazione: UNIVERSITA' DEGLI STUDI DI MESSINA/80004070837
Prof.ssa Clara Enza Urzì

Co-Tutor
Dott.ssa Nadia Ruocco
SZN-CRIMAC
Nadia Ruocco
Firmato digitalmente da Nadia Ruocco
Data: 2025.07.01 12:19:48 +02'00'

Co-Tutor
Dott. Silvestro Antonio Ruffolo
UNICAL
Silvestro Antonio Ruffolo
30.06.2025 19:59:04 GMT+02:00

Co-Tutor
Dott. Christian Galasso
SZN-CRIMAC
Firmato digitalmente da GALASSO CHRISTIAN
C=IT

Ciclo XXXVII A. A. 2024/2025

Table of contents

ABSTRACT

Underwater cultural heritage (UCH) faces numerous threats that endanger its conservation. The deterioration of submerged stones artifacts starts for a concurrence of physical-chemical events such abrasion, deposition, oxidation, and reduction, as well as biological factors such as microorganisms, and later on, macroorganisms colonization. Due to environmental conditions, *in situ* protection of UCH poses serious issues and the current methods suggested by the 2001 UNESCO convention result inefficient for the long-time conservation of archaeological sites. One of the main problems is biodeterioration due to microbes present in the underwater environment. During my PhD research activities, within the framework of the CRIMAC-UNALTERABLE project, investigations were carried out in order to test anti-biofouling ecofriendly coatings to protect the underwater stone cultural heritage. Therefore, a coating based on a mixture of surfactant ionic liquids (IL), which gave excellent results in the protection of terrestrial CH was chosen. The activities were initially aimed at characterizing the physical properties of IL-treated Carrara marble and limestone probe surfaces in association with various silica consolidants and their persistency in water environments through UV-daylight weathering and washing tests. Finally, the antifouling behavior was evaluated after exposure of treated and untreated in coastal marine environment for 1 year. Each tested condition was sampled at increasing time intervals (24 hours, 1, 6, and 12 months). Biodeterioration processes and antifouling activity of the IL based coatings were studied at each time point by microscopic analysis (stereo-microscopy, CLSM and SEM) and DNA metabarcoding. Seawater and sediments samples were also studied to monitoring the dynamics of the surrounding environment that affected surface biofouling processes.

The use of coatings based on ionic liquid technology combined with current commercial silica-based consolidants has demonstrated an effective increase in durability of coatings applied to marble surfaces exposed in a marine environment by slowing down surface biofouling. However, the two-step applied coating results in less durability on more porous limestone surfaces, while the monolayer coating homogeneously penetrates below the first layer of the stone surface interfering with the foulers' interaction to the surface and decreasing their biodeteriorating action.

FOREWORDS

Human activities have contributed to the accumulation of underwater cultural assets, which are crucial for understanding past human interactions in coastal areas throughout history. Investigating traces of these activities across various time periods offers valuable insights into the evolution of societies and their relationships with the sea. According to UNESCO "*underwater cultural heritage is defined as all traces of human existence of a cultural, historical, or archaeological nature that have been partially or totally immersed for at least 100 years. Protection and preservation of UCH allow for better knowledge and appreciation of past culture, history, and science*" (Öniz et al., 2024). Underwater archaeology has gained an increased interest in the last decades in order to preserve these submerged treasures. Biologists, ecologists, geologists, chemists, conservation scientists, as well as all operators working in the underwater sector have focused their studies on the knowledge, management and protection of underwater sites. The heritage submerged in marine environment suffers threats of different nature and the resulting damage mainly depends on the cultural heritage's material component and exposure conditions that can be extremely diverse and mutable (Ricca and La Russa, 2020; Sacco Perasso et al., 2022). Seasonal climatic variations, erosion and abrasion by currents, tidal movements or changes in water circulation represent the main mechanical threat to cultural heritage. The deterioration of submerged stones artifacts is a process that starts from both physical-chemical events of abrasion, deposition, oxidation, and reduction, and biological factors such as microorganisms' colonization. Chemical attack is caused by oxidation and various types of ionic corrosion due to oxygen dissolved in water, but the aggression exerted by micro- and macro-organisms represent the most critical threat to submerged stone materials (Crisci et al., 2010). The bioerosion process starts as soon as a stone material is in contact with the aquatic environment and is named "*marine biofouling*" (Callow and Callow, 2002). Submerged inorganic materials in marine environments undergo rapid colonization by microorganisms, forming an organic conditioning film consisting of dissolved organic molecules (e.g., carbohydrates, proteins, and uronic acids) (Callow and Callow, 2002). This initial layer facilitates the settlement of microorganisms that are present in sediments and seawater. Bacteria and algae settle and produce a biofilm matrix composed of extracellular polymeric substances (EPS), including polysaccharides, proteins, glycoproteins, glycolipids, and extracellular DNA (López-Arce et al., 2013; Aloise et al., 2014). The biofilm represents a refuge for microorganisms. Its composition varies depending on environment physicochemical parameters like temperature, pH, depth, and associated

bacterial community (Persat et al., 2015; Flemming et al., 2016). Prolonged exposure leads to complex communities of microbes, plants and animals resulting in macrofouling. Microorganisms and associated biofilms are pivotal influencers of settlement dynamics and recruitment patterns of macrofoulers. Microfoulers transform surfaces and emit chemical signals, either beckoning or discouraging potential settlers (Lam et al., 2003; Dobretsov et al., 2013; Mieszkin et al., 2013). Biofilm characteristics, such as age, density, composition and bacterial cooperation, play a critical role enhancing surface adhesion and environmental persistence (Hadfield, 2011; Wang et al., 2012; Flemming et al., 2016; Muhammad et al., 2020).

Biofouling processes that take place on submerged marble and limestone surfaces result in deterioration as microboring, pitting, and macroperforations (Callow and Callow, 2002; Ricci et al., 2009; La Russa et al., 2013; Aloise et al., 2014). The latter are often caused by molluscs as *Lithophaga lithophaga* and *Gastrochaena dubia,* which facilitate colonization by endolithic sponges (Ricci et al., 2009). Serpulids and bryozoans can cause unesthetic calcareous encrustations on lithic surfaces, but boring sponges are among the most aggressive biodeteriogens (Ricci et al., 2009; Crisci et al., 2010; La Russa et al., 2013; Aloise et al., 2014). Therefore, the biodeterioration of stone materials is also dependent by the intrinsic characteristics of the stone, such as texture, composition, mineral properties, porosity, hardness and strength of materials (La Russa et al., 2015). Different materials underwater may show a different degree of response to biological colonization. For instance, submerged ignimbrites and bricks seem to be materials that are more resistant to biological colonization, while marble is subject to microbial adhesion(Aloise et al., 2014; Ruffolo et al., 2013). The 2001 UNESCO Convention is the main international framework the safeguarding underwater archaeological sites. The Annex contains the "*Rules concerning activities directed at underwater cultural heritage*" which provide guidelines for proper *in situ* protection of UCH (UNESCO, 2001). On the whole, it suggests the use of safe methods to ensure that cultural heritage is better preserved, restored and can be displayed to the public while limiting the damage caused by human intrusion (Thijs, 2013). However, the techniques fully endorsed by the members of the Convention's Scientific and Technical Advisory Body are often site-specific and variable in effectiveness. Diagnostic analysis of the conservation status of cultural heritage is essential to determine the best approach (Aloise et al., 2014). *In situ* assessment captures contextual information about artifact's history and environmental conditions (Salaris

et al., 2008). For this reason, the UNESCO Guidelines prioritizes *in situ conservation*, but exceptions are allowed. Artifacts may be removed for justified reasons and research needs and stored in humidity-controlled environments during documentation to prevent degradation (Thijs, 2013; Alvik, 2018). Post-study *reburial of archaeological material* in seabed trenches or engineered structures enhances material stability in natural environments, mitigating physical, biological, and chemical deterioration (Bekić et al., 2011; Ortmann, 2014). Studies conducted on submerged marble artefacts define the burial as a potential protection strategy against deteriorating agents in the underwater environment (Davidde et al., 2010; Ricci et al., 2013). In other cases, the analysis should be carried out *in situ*, followed by correct intervention procedures in underwater restoration. Natural sand coverage often acts as a physical protective barrier, but changing sea conditions, wave motion and currents may expose the site again to environment deterioration agents. This natural protection method can be stabilised using barriers such as bulwarks or artificial sea grass. *Artificial seagrass* is used to promote sediment deposition, as natural seagrass does not easily recover or re-establish on sandy substrates once it has been disturbed (Grenier et al., 2006). However, this technique in not always successful, especially in low-energy marine environments (Skowronek et al., 1987). *Geotextiles* are often used together with sand burial to isolate research areas before covering them with sand, avoiding contamination and damage of archaeological site. The development of a compact layer of fine sediments acts as a physical barrier and textile fibres show resistance to biodeterioration by marine microorganisms up to 12 years (Pournou, 2018). *Sandbags* are useful for consolidating archaeological sites most exposed to erosive agents. Polypropylene bags filled with sand are placed to cover sites and to resist tidal currents (Grenier et al., 2006). However, this is not a permanent solution as the bags deteriorate over time and require regular monitoring. Coverage of endangered sites with *polypropylene nets* has proven to be the best solution for resistance and longevity. The netting is fixed with sandbags or spikes and allows an artificial deposit to accumulate over time, protecting the site from external agents. However, this technique requires specific current and sediment conditions and can be blocked by the growth of marine organisms on the net (Bekić et al., 2011). The *closed-box* system provides long-term *in situ* protection isolating sites from human threats like theft, pollution, and intentional or unintentional mechanical damage. A permanent metal structure, adaptable for archaeological research access, is installed on protected area and covered with sand, protective nets, stones, and grass to mask the site by merging it into

its natural environment (Bekić et al., 2011). This approach minimizes structural stress on artifacts while reducing biofouling through light deprivation, resulting in less aggressive artifacts deterioration (Davidde, 2004). However, this method is particularly efficient for shipwrecks and compact - closed structures. Another technique approved by the 2001 UNESCO Convention consists in the use of *protective cages* anchored to the seabed allowing public presentation without compromise of safety. The net is preserved by a protective coating combined with zinc protectors that corrode before the steel cage (Mesic´, 2008). The efficacy of the method is currently estimated up to about twenty years, but effectiveness depends on seabed substrate characteristics, as variable conditions influence structural stability (Salaris et al., 2008; Bekić et al., 2011).

While useful for site stabilization, these techniques are insufficient for long-term preservation combined with public access. Therefore, there is a growing focus on eco-friendly antifouling coatings, a more ambitious but promising approach. The great challenge is the development of innovative protocols that respect eco-sustainability criteria. Solutions discussed in scientific literature to prevent biological growth on stone surfaces are limited and often toxic and harmful for humans and for ecosystems. Available antifouling products are mainly designed for the protection of ship hulls and are not easily adaptable to archaeological materials.

Recently, in the frame of CoMAS project, siloxane waxes containing nanopowders of titanium dioxide mixed with silver have been patented as an antifouling solution for submerged stone surfaces and applied directly in the underwater environment on Carrara marble and tuff samples placed in the area of Campi Flegrei (Ruffolo et al., 2017). However, despite a good performance of the treated samples when compared to untreated probes (La Russa et al., 2015; Bruno et al., 2016) after 1 year, scarce or none persistency of the wax treatments was evident, and after 20 months fouling formation occurred again (Ruffolo et al., 2017). The use of nanoparticles as antibacterial agents, although promising, raises issues related to their possible environmental dispersion, which require careful evaluation (Cirone et al., 2023). These results underscore the need for coatings designed specifically for underwater use, combining ecological safety and increased stability in marine conditions.

INTRODUCTION

Current research regarding a suitable coating for CH, focuses on methods that should match the “green criteria” taking into account the concepts of ‘Safe by Design’ (Semenzin et al., 2019; Lo Schiavo et al., 2020). This means that conservation products/processes must meet criteria such as reversibility, bio-receptivity and biodegradability. In this context, bio- and nano-technologies have provided a significant contribution. In particular, in the past 20 years, ionic liquids (ILs) have gained importance as a potential sustainable solution due to their tuneable physico-chemical (Xin and Hao, 2014; Cardiano et al., 2015) and biological properties (Pendleton and Gilmore, 2015). ILs have very low volatility, thermal and chemical stability, conductivity, high heat capacity, low melting point (<100°C) and remarkable electrochemical potential (Seddon, 1997, 2003; Welton, 1999; Wasserscheid and Welton, 2007). Moreover, their ionic nature makes them synthetically manageable and suitable for applications across many fields (Misra et al., 2018). Bioactivity is related to their amphiphilic property (Borkowski et al., 2019). The length of the alkyl chain plays a key role in antibacterial efficacy, with longer chains improving activity up to a critical point (Petkovic et al., 2011; Jordan and Gathergood, 2015). Studies on imidazolium-based ILs with alkyl chains characterized by an excess of 10 carbon atoms show a lipophilicity/antimicrobial activity relationship. The choice of long chains and regulation of the head group allows ILs interaction with bacterial membranes disrupting the lipid bilayer and compromising the cell's integrity (Egorova et al., 2017). The synthesis of neutral and ionic hybrid compounds containing ILs terminal sections combined with diaminothiadiazole or 1,2,4-triazole as Schiff-bases showed broad bactericide efficacy and excellent antibacterial effects against various marine bacteria. These hybrids were used to develop anti-biofouling coatings that prevent the invasion and adhesion of marine organisms, especially red algae, tube worms, and zooids (Elshaarawy et al., 2016). Laboratory tests showed that IL-based Schiff-bases inhibited the growth of common marine microorganisms. When incorporated into commercial paint matrices and applied on polyacrylic panels, they showed an enhancement of antifouling performance, although only up to 5 months after immersion. These compounds are therefore regarded as promising additives for the next generation of antifouling coatings (Fallah et al., 2021). The careful combination of naturally occurring ions, such as cholinium, morfolinium amino acids and drug anions, has resulted in so-called “*ILs of third generation*” (Ferraz et al., 2011; Petkovic et al., 2011). Among these, Surface-Active Ionic Liquids (SA-ILs) with choline-based cations and dodecylbenzenesulfonate (DBS) or halide anions demonstrated

antimicrobial/antifouling activity when applied on limestone and marble surfaces (De Leo et al., 2021).. Evaluation of the antifouling activity of ionic species was conducted on stone surfaces non-inoculated and inoculated with microbial suspensions of strains isolated from deteriorated stone material. Nanosilica suspension was used to consolidate the stone surfaces and promote ionic liquid adhesion. SA-ILs consisting of N-(2-Hydroxyethyl)-N,N-Dimethyl-1-Dodecanaminium Bromide and N-(2-Hydroxyethyl)-N,N-Dimethyl-1-Dodecanaminium Dodecylbenzenesulphonate showed the best performance on inoculated surfaces. Replacing the halide anion with DBS gave a preventive function reducing spontaneous microbial colonization. The antimicrobial effect of these SA-ILs has been linked to their amphiphilic structure, enabling them to penetrate and damage microbial membranes (Borkowski et al., 2019). This mechanism is comparable to that of traditional surfactants, particularly long-chain cationic surfactants (C10–C14), which are known to disrupt cellular membranes through the insertion of hydrophobic tails into lipid bilayers (Liao et al., 2025). Given that ionic liquids are composed of complex anions with surface-active features, their biocidal activity is thought to arise from similar membrane-targeting interactions. By incorporating surfactant moieties within the cation@anion pair, their bioactivity was modulated and optimized for use in cultural heritage conservation (De Leo et al., 2017). The long-term behavior of these ILs was also evaluated in terrestrial environments. Results showed a very scarce spontaneous colonization on treated surfaces compared to both untreated controls and those treated with nanosilica alone (Alì, 2025; Ali et al., in prep.). Based on these promising outcomes, this research project, within the frame of CRIMAC-UNALTERABLE, proposed the use of IL-based coatings for underwater applications. A synergic effect was hypothesized between the two ionic species and various consolidants/water repellents, aimed at improving efficiency and suitable application for underwater CH.

AIM

The aim of the present PhD research activities was to test more innovative and eco-sustainable coatings for the protection of submerged stone cultural heritage through a multidisciplinary approach that involved the experiences of three operative units: the Stazione Zoologica Anton Dohrn, Calabria Marine Centre in Amendolara (CS), the University of Calabria (UNICAL) in Rende (CS) and the University of Messina (UNIME).

A mixture of *ILs of the third generation, based on SA-active cholinium cation,* already succefully tested in terrestrial environment were used in combination to different silica consolidants. The investigation focused on the physical properties of treated stone surfaces, the durability of the coatings in submerged environment, and the evaluation of their antifouling performance following immersion in marine setting for 12 months. The analysis of untreated stone surfaces, as well as seawater and sediment samples from the exposure site, was essential to explore and better understand the mechanisms of biodeterioration and the interactions between biofoulers and inorganic materials, which remain poorly studied in the current literature. At the same time, the mid-term exposure of treated specimens and their sampling at increasing time intervals made it possible to assess the antifouling activity of the coatings and to evaluate their potential applicability for the long-term protection of underwater cultural heritage.

CHAPTER 1

CHEMICO-PHYSICAL CHARACTERIZATION OF STONE PROBES TREATED WITH IL-BASED COATINGS

INTRODUCTION

The "third-generation ILs" are based on natural and biodegradable ions (cholinium, morfolinium, aminoacids, drug anions) (Petkovic et al., 2011). Few data are currently available to support the antimicrobial potential as preservation products (De Leo et al., 2017; Lo Schiavo et al., 2020). In 2021, De Leo and co-workers developed a series of surface-active ionic liquids (SA-ILs) (De Leo et al., 2021). The engineered molecules were characterized by mono- and di-choline cations with alkyl chains of different lengths and as anions conventional halide or the surfactant dodecylbenzenesulfonate (DBS). Among the tested compounds, two SA-ILs based on cholinium cations combined with bromide and on DBS anions exhibited antimicrobial activity in laboratory conditions and a preventive effect against spontaneous colonization when applied on stone surfaces (De Leo et al., 2021). These coatings remained effective on stone probes for extended periods, with data indicating antifouling efficacy lasting over 5 years. (Ali doctorate thesis 2025, Ali et al., in prep). To improve their overall performance, a series of formulations was developed by combining cholinium cations and bromide and DBS anions in varying molar ratio (1:1, 1:3, and 3:1). The design of these ionic liquid mixtures was based on established principles of surfactant–membrane interactions, which suggest that synergistic effects can arise from the combination of surfactants with complementary mechanisms of action (Liao et al., 2025). In particular, it was hypothesized that the inclusion of the cationic surfactant bromide could potentiate the antimicrobial activity of DBS, provided the formulation was properly balanced. Among the tested compounds, the 3:1 cholinium@bromide-DBS mixture (IL) demonstrated the most promising antimicrobial activity in agar diffusion tests and was therefore selected for subsequent evaluations (Luci et al., 2023). These preliminary investigations focused on assessing the behavior of stone surfaces treated with IL mixture under exposure to deteriorating agents present in underwater environment, for the purpose of valuating its suitability as a coating for UCH protection.

MATERIALS AND METHODS

Preparation of stone probes

Locally available San Lucido limestone and Carrara marble were used as stone material for the experimental work. The choice of these materials was driven by their widespread discovery in the submerged cultural heritage and their known susceptibility to biodeterioration (Ricci et al., 2009; Crisci et al., 2010; Aloise et al., 2014; La Russa et al., 2015). From a mineralogical point of view, both lithotypes were mainly constituted of calcite. The marble surfaces appeared homogenous with a low porosity (approximately 2 %), the limestone had an accessible porosity of about 17 % and contained a small portion of dolomites (< 2 %) (Veltri et al., 2019). The stone blocks were cut into 5 × 5 × 2 cm^3 and 2.7 × 2.7 × 1 cm^3 specimens. The total number of samples was calculated based on the number of conditions evaluated, three replicates for each condition and number of tests to be performed. Before treatment, all specimens were washed with a brush and bidistilled water and dried in the oven for 24 h at 80 °C.

The 5 × 5 × 2 cm^3 specimens were subjected to three different coating conditions. Two involved bilayer treatments with a first layer of silica-based consolidant, Nano Estel (NES, CTS srl Altavilla Vicentina, Italy) or Estel 1000 (ES, CTS srl Altavilla Vicentina, Italy), followed by a top layer of IL; the third condition was a monolayer treatment made of pure tetraethyl orthosilicate mixed with the IL. For bilayer coatings, NES was diluted in two parts of bidistilled water before application and the treated surfaces had a setting time of 4 days, whereas ES was applied to the surfaces without further dilution and left to dry at room temperature for 4 weeks, as suggested by the producers. IL, characterized by mixture of N-(2-Hydroxyethyl)-N,N-Dimethyl-1-Dodecanaminium cations and bromide and DBS anions in the molar ratio 3:1, was then applied to the pre-treated specimens (Figure 1).

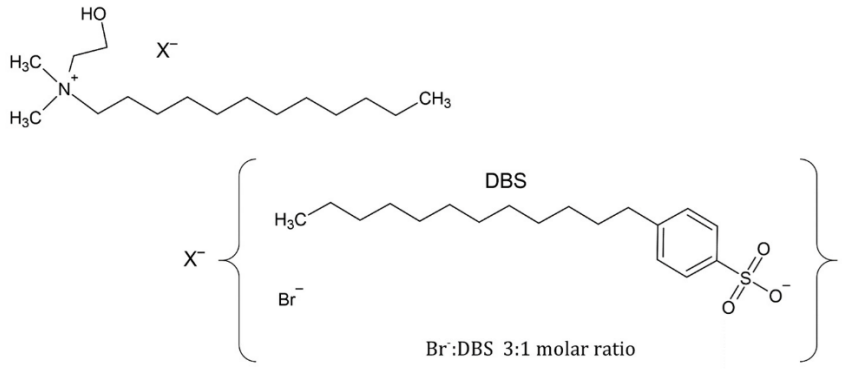

Figure 1. Chemical structure of the used ionic liquid mixture (IL)

The IL were obtained following the procedure already adopted for the synthesis of analogous cholinium - based ionic liquids (De Leo et al., 2021). In brief, a methanol suspension (30 mL) of NaDBS (0.82 g, 2.34 mmol) was added to a solution (170 mL) of the N-(2-Hydroxyethyl)-N,N-dimethyl-1- dodecanaminium bromide in the same solvent (3.17 g, 9.375 mmol). The resulting mixture was stirred for 12 h and then left at 10 °C for 3 h. The IL containing "mother liquors" was pipetted off and then diluted to 250 mL to reach a concentration of ca. 0.0375 M in cholinium-based cation. Before use, the resulting IL mixture was subjected to intense ultrasonic bath sonication to avoid significant aggregation phenomenon. DLS measurements revealed the presence of agglomerations even at concentration of 0.4 mM, (work in progress), consistent with the presence of surfactant species, but IL methanol mixture appears transparent at the naked eye. After application, it was left to dry at room temperature for 24 hours (NES + I; ES + I). Concerning the monolayer treatment, coating was obtained by adding 50 ml of absolute ethanol to 73 g of TEOS (77.6 mmol) in 250 ml of IL (TE + I). The mixture was again subjected to intense ultrasonic bath sonication for two minutes and then applied to the stone surfaces, which were left to dry at room temperature for 4 weeks (Figure 2).

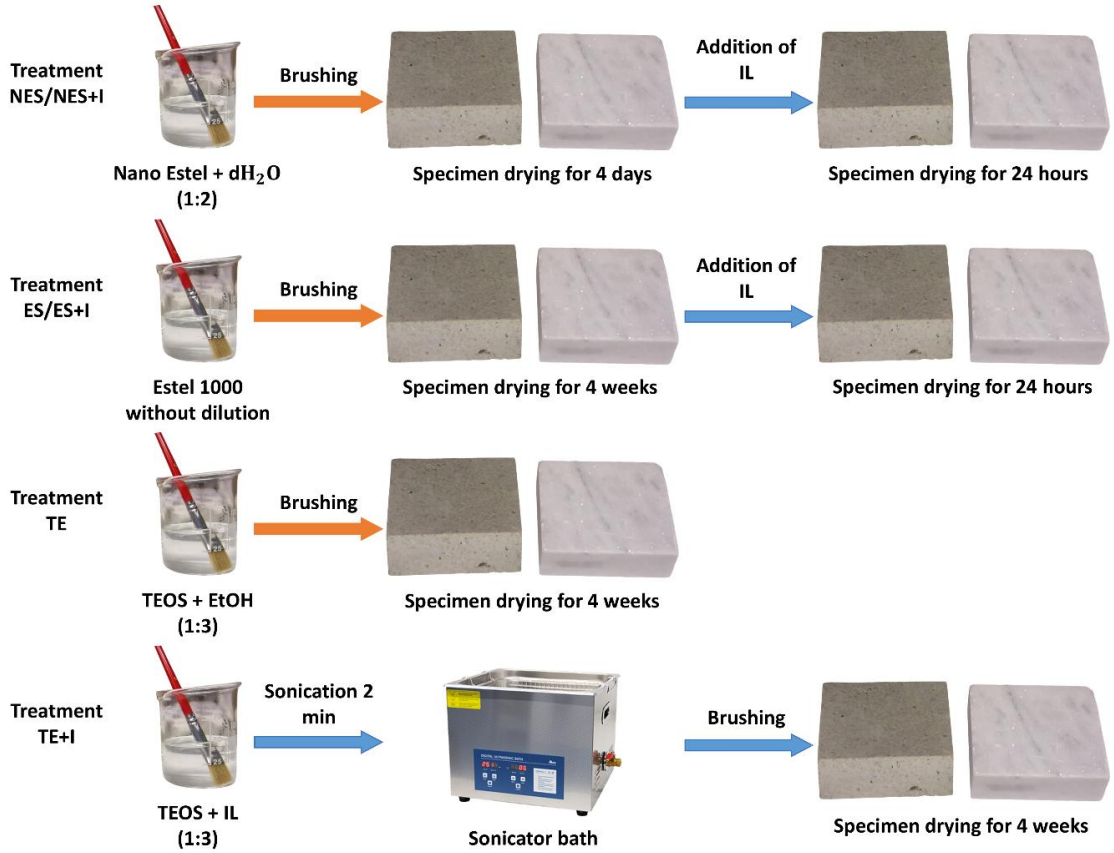

Figure 2. Schematization of bare and IL-consolidant bilayer/monolayer treatments: Nano Estel/Nano Estel + IL (NES/NES+I); Estel 1000/Estel 1000 + IL (ES/ES+I); TEOS alone (TE) and TEOS + IL (TE+I).

The specimens with a size of 2.7 × 2.7 × 1 cm^3, used for *washout and microcosm tests*, were treated following the same procedures replacing IL with IL Pyrene-1-sulfonate derivative (I-PyrS). I-PyrS was used to verify the distribution and presence of IL on surfaces, as the product emits fluorescence when exposed to UV light. The tagged coating was obtained adding 0.074 g (0.45 mmol) (ca. 6 % by mol) of sodium Pyrene-1-sulfonate to a methanol mixture (200 mL) of IL (concentration 0.0375 M). The resulting mixture was left under stirring overnight and then applied without further work-up.

All coatings were applied by brush and summary of the treatments is reported in Table 1.

Table 1. Summary of treatments with IL (N-(2-Hydroxyethyl)-N,N-dimethyl-1- dodecanaminium Br: DBS 3:1) and I - PyrS (IL- Pyrene-1-sulfonate).

Lithotype	ID	Binder			IL / IL-PyrS	
		Product	Amount (g/m^2)		Application	Amount (mmol/m^2)
			Product	Active matter		
Marble	**Untreated**	-	-	-	-	-
	NES	Nano Estel	80	12	-	-
	NES + I/I - PyrS	Nano Estel	80	12	Top layer	0.57
	ES	Estel 1000	80	60	-	-
	ES + I/I - PyrS	Estel 1000	80	60	Top layer	0.57
	TE	TEOS	80	24	-	-
	TE + I/I - PyrS	TEOS	80	24	Mixed with binder	0.57
Limestone	**Untreated**	-	-	-	-	-
	NES	Nano Estel	160	24	-	-
	NES + I/I - PyrS	Nano Estel	160	24	Top layer	1.14
	ES	Estel 1000	160	120	-	-
	ES + I/I - PyrS	Estel 1000	160	120	Top layer	1.14
	TE	TEOS	160	48	-	-
	TE + I/I - PyrS	TEOS	160	48	Mixed with binder	1.14

Chemico-physical characterization properties of stone probes

Characterization tests were performed on untreated and treated surfaces with bare binders and after application of the IL.

- *Colorimetric measurement* procedures were in accordance with the guidelines provided by UNI EN ISO/CIE 11664-4:2019 (ISO/CIE 11664-4:2019). The measurements were carried out at 5 points on the surface with the ZL 310 colorimeter. The coordinates L*, a* and b* provided by the instrument were incorporated into the CIE system. L* is brightness index (0 = absolute black, 100 = absolute white) and a* and b* are chromaticity coordinates (a* is the position between green (a* < 0) and red (a* < 0); b* is the position between blue (b* < 0) and yellow (b* > 0). The colour variation of the surfaces was calculated by replacing the obtained

values in the following formula: $\Delta E = (\Delta L^{*2} + \Delta a^{*2} + \Delta b^{*2})^{1/2}$. Colorimetric analysis was performed before and after treatment and after aging. Different specimens treated with the binder alone and treated with IL-based coatings were prepared for UV aging. The values of ΔE obtained from the investigation on the replicates' surface of the same tested condition were averaged to obtain a single value and standard deviation.

- *Contact angle* tests were carried out to evaluate the degree of hydrophilicity/hydrophobicity of the treated surfaces. Measurements were performed with LSA LAUDA Scientific Surface Analyzer System according to the regulatory standard of static contact angle measurement (ISO/CIE 15802:2010). All marble and limestone samples were analyzed before and after binder treatment and after addition of IL. The investigation was also repeated on the untreated and treated samples with bare binder and with IL-based coating after UV-daylight weathering. The contact angle measurement was taken at 5 points on the surface of each sample in order to be indicative of the behavior of the whole surface. The average value of the measurements was in turn averaged with the average value obtained from the replicates of the same condition. This resulted in a single value and standard deviation for each condition tested.

- *Capillary water absorption* tests were carried out according to UNI EN 15801:2010 (ISO/CIE 15801:2010). The test allowed the evaluation of possible variations in the amount and speed of water absorption between untreated and treated specimens with the different coatings containing the ionic species. The investigation was performed on treated marble and limestone specimens with the coatings containing the ionic liquids and on the same after UV-daylight weathering. A layer of absorbent paper about 1 cm thick was placed in the bottom of a container. Demineralized water was added to the container until the absorbent layer was saturated. The specimens were weighed and placed on the laying bed with the test surface in contact with the wet paper. The specimens were removed from the support and weighed after 10, 20, 30 and 60 min and after 4, 6, 24, 48, 72 and 96 h. After 5 days from the start of the trial, the test was stopped because the specimens showed a saturated state. The amount of water absorbed by the sample as a function of time is expressed as the difference between the mass of the specimen at time t_i and the mass of the dry specimen in relation to the surface area in contact with water ($Q_i = [(m_i - m_0) / A$). Next, the Q_i values of the replicates of the same condition were averaged to obtain a single value and standard deviation.

Laboratory evaluation of coatings durability

Coating durability was evaluated with different methods as reported below.

UV aging

UV aging tests were performed on untreated and treated marble and limestone samples with bare binder and binder bonded to the IL. Samples placed in SUNTEST XLS+ chamber were subjected to the action of an artificial daylight fluorescent lamp combining visible and UV emissions (λ = 300-800 nm, irradiance = 500 W/m^2) for 507 hours at a temperature of about 35 °C. At the end, all samples were subjected to chemico-physical characterization of the stone probe properties. The investigation verified the durability of the coatings when exposed to UV irradiation, evaluating any forms of degradation that could take place on the treated surfaces, such as brightening or yellowing. In order to verify the stability, the IL was subjected to analysis by IR spectroscopy. The investigation was carried out on the coating at the end of the setting time and after UV aging. Glass Petri dishes 70 mm diameter were washed with acetone, left to evaporate under hood at room temperature. The surface of the dish was then covered with IL by brush, applying the same amount of coating as used for the treatment of the limestone material shown in Table 1. The dishes were left to dry under hood overnight and then subjected to artificial daylight radiation by a SUNTEST XLS+ chamber at same parameters settled for UV aging of treated stone specimens. At the end, part of the coating was scratched from the surface and subjected to IR spectroscopy. The spectrophotometer used was a Perkin Elmer Spectrum 100, equipped with an attenuated total reflectance (ATR) accessory. Infrared spectra were recorded in ATR mode, in the range of 500 – 4000 cm^{-1} at a resolution of 4 cm^{-1}.

Washout and microcosm tests

Marble and limestone samples were treated with I-PyrS, sterilized under UV light for 30 minutes in an inverted position, followed by an additional 2 hours with the test surface in direct contact with the radiation. This procedure ensured that the entire surface of the probes was sterilized.

For *washout tests*, the samples were placed in closed systems that allowed contact with sterile seawater to test the effective action of washout in absence of microorganisms. Each sample was placed inside 120 mL screw-cap sterile container and 80 mL sterile seawater was added. The seawater had been previously prepared through vacuum filtration using a Stericup system

and then sterilized in autoclave at 121 °C for 20 min. The resulting systems were incubated for 6 months in thermostatic shaker incubator at 20 °C with rotating speed 100 r/min. In parallel, samples were exposed in a controlled *microcosm* as described below. The microcosm was a closed system that made possible to evaluate the resistance of the coatings in an environment more similar to the real marine environment and in presence of marine microorganisms, before any real exposure. Laboratory tanks (30 × 47 × 28 cm^3) containing seawater from an external transport system that connect the tanks to the coastal sea was used. The seawater was filtered through a sand filter and skimmer. Next, the seawater was clarified with UV treatment (Helix Max 2.0 UV steriliser) and the organic residues were oxidised with ozone (ozone 30-400-manual). The tank was filled with ~ 40 L of seawater treated with the external system just described, and then it was only subjected to internal recirculation. Each closed-system tank was equipped with a water recirculation pump through mechanical filtration and biological purification systems. The temperature of the seawater inside the tank was maintained at about 19.5 °C and the salinity at about 37.4 ppm over the course of the test. At increasing intervals of 15 days, 1, 3 and 6 months, three replicates of marble and limestone samples treated with silica@I-PyrS coatings and exposed in the two conditions just described were analyzed. The samples were washed with bidistilled water and weighed. After drying in the oven for 2 h at 40 °C, the samples were weighed again to check for complete removal of moisture. Finally, pictures were taken under UV light.

Scanning Electron Microscopy (SEM)

After UV visualization Micro-morphological features of I-PyrS-treated limestone surfaces washed out for 3 months were explored by SEM, specimens were metallized with graphite and visualized with Ultra-High-Resolution SEM (UHR-SEM) - ZEISS CrossBeam 350 equipment, coupled with the EDS-EDAX OCTANE spectrometer. Investigation was carried out by X-ray energy dispersive (EDX) and back-scattering electron (BSE) techniques.

RESULTS AND DISCUSSIONS

Chemico-physical characterization properties of untreated, treated and aged probes

Colorimetric variations

Colorimetric measurements showed that the IL-treatment of marble and limestone surfaces caused a colorimetric variation of less than 5 (Figure 3). This value is typically regarded as a threshold beyond which color variation becomes perceptible to the naked eye, therefore unacceptable in the field of cultural heritage conservation.

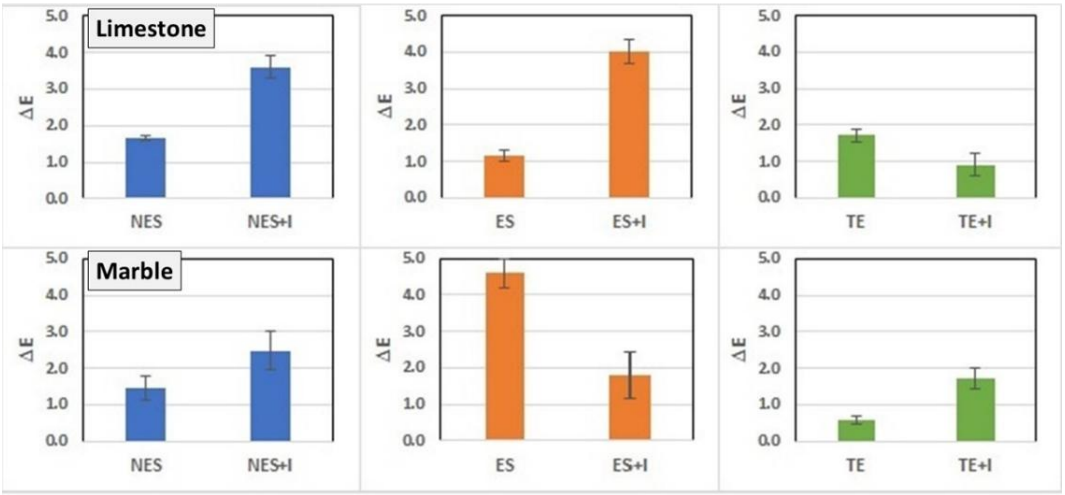

Figure 3. Colorimetric differences between untreated and treated specimens.

Treatment of limestone surfaces with binders alone induced a color variation of less than 2. Addition of IL on Nano Estel and Estel binders makes the variation slightly higher, but still under the threshold limit. On the other hand, treatment of marble surfaces with Nano Estel and TEOS alone induced a color change of less than 2 and the addition of IL caused a slight increase in the variation by about 1 unit. A different behavior was found for the Estel treatment. The bare binder induced a stronger color variation of about 4.5. A more detailed analysis, considering the individual components (L*, a*, and b*), indicates that the L* coordinate have the most significant impact on the Delta E value (Figure 4).

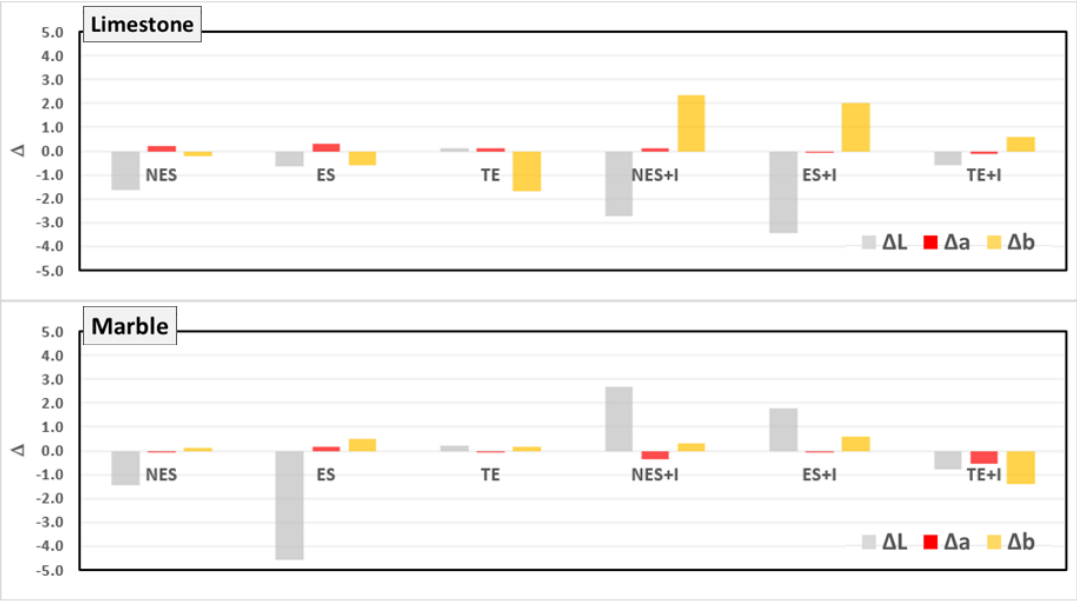

Figure 4. Components ΔL, Δa, Δb of ΔE value for each treatment.

In particular, for Estel treatment of marble samples, L* values decreased by about 4 units, as did the L* coordinate for treatment with Nano Estel and Estel with IL addition on limestone, where L* values decreased by about 3 units. For the treatment of marble probes with Estel binder alone, the variation is likely caused by a wetting effect attributable to the solvent of the consolidant that remains trapped into the stone as the ethyl silicate cures (Manoudis et al., 2009). This effect is temporary, although it can persist for several months following the treatment. On limestone, the addition of IL as top layer causes darkening of the surfaces that results in colorimetric variation, attributable to the higher porosity of the material compared to marble surfaces. The analysis of colorimetric variations between treated and aged surfaces can provide information about the effects of UV-daylight radiation on the treated surface. A variation of ΔE below 1,5 was detected for all treatments of limestone surfaces. On the other hand, aged marble surface treatments showed a variation of ΔE value below 3.5 (Figure 5).

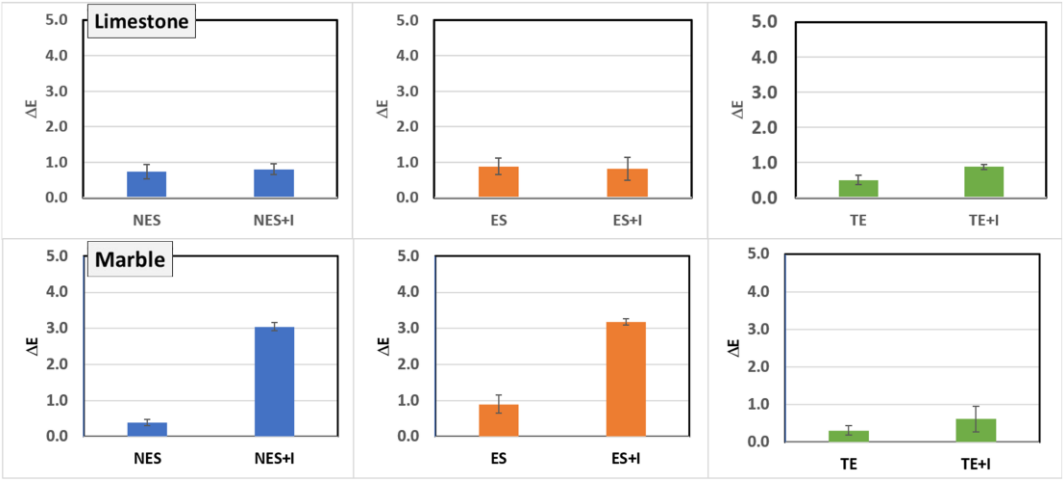

Figure 5. Colorimetric differences between aged and treated specimens.

In the case of marbles, binders combined with IL suffered a higher variation than the bare binder. The color resulting after TE+I treatment is less affected by UV radiation. This is likely because the IL was not applied on the surface in a two-step process; instead, it was present in bulk due to being applied all at once. Looking at the single components (ΔL, Δa and Δb) of the ΔE value for each treatment applied to marble surfaces, again the L* coordinate is the most variable (Figure 6). It is important to note that, for NES+I and ES+I, the L* coordinate moves in the opposite direction compared to treated-untreated variation shown in Figure 4. This is a result of the coating equilibrium processes triggered by UV-daylight radiation.

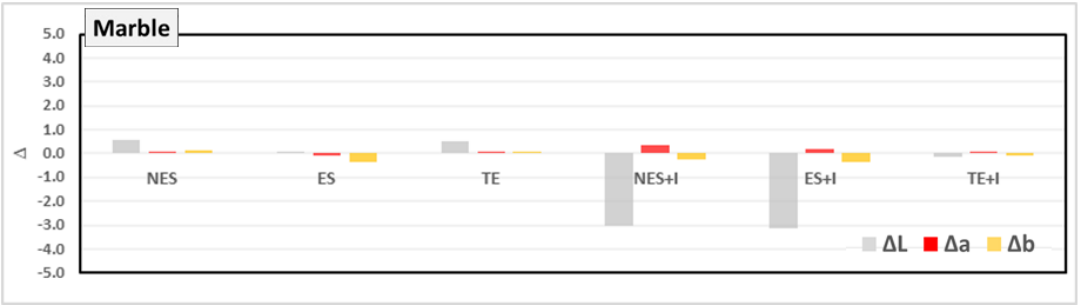

Figure 6. ΔE value with its components (ΔL, Δa, Δb) for each treatment on marble surfaces.

Contact angle measurements

The contact angle measurements on the treated marble and limestone specimens are reported in Figure 7. The untreated marble specimen shows a contact angle of about 40°; it is 0 on untreated limestone specimens.

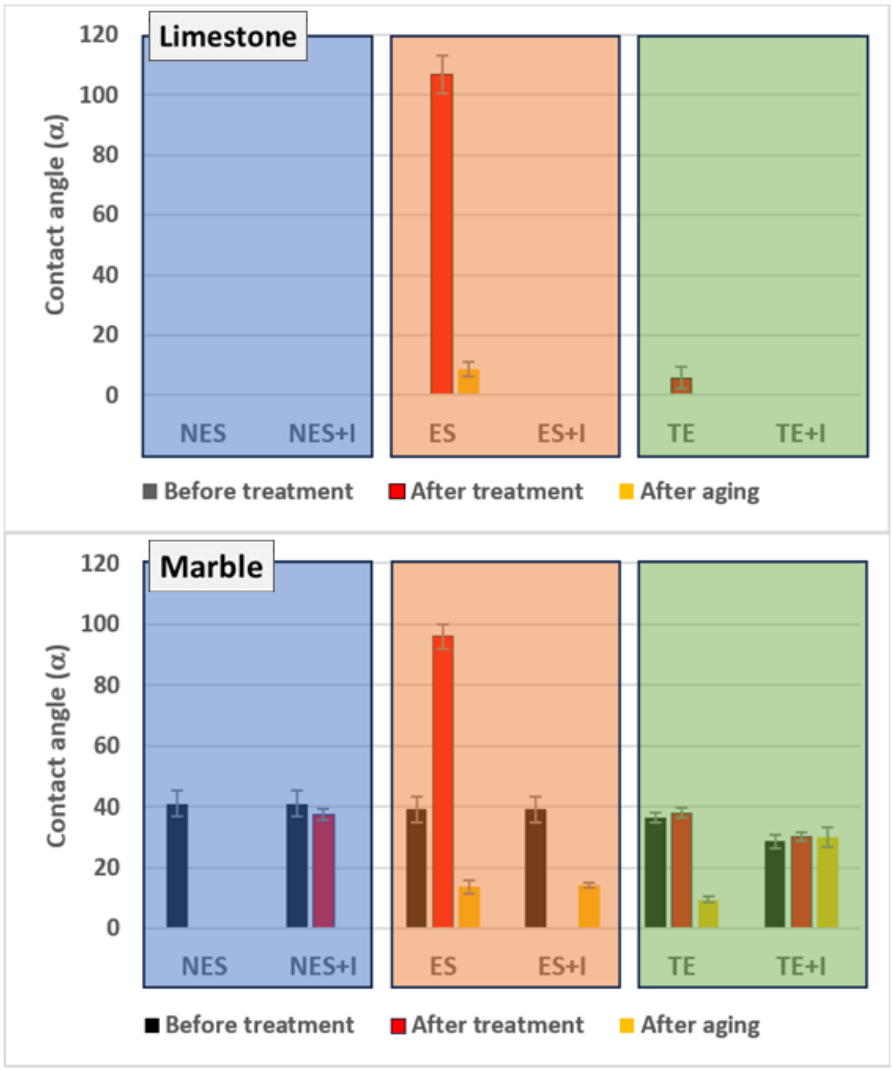

Figure 7. Contact angle measured for untreated, treated and aged samples (in blue it has been highlighted the treatments with Nano Estel binder, in orange those with ESTEL 1000, in green those with TEOS)

The NES and NES+I treatments do not alter the hydrophilic nature of limestone surfaces. A different behavior is observed for marble specimens; NES treatment makes the surface hydrophilic. This is attributed to the nanosilica which, upon curing, leaves a negative charge on its surface due OH groups (De Leo et al., 2021). An interesting behavior is observed after IL application, as the NES + I treatment of marble surfaces exhibits a wettability similar to that of the untreated ones. Considering the ionic nature of IL, it is reasonable to assume that

it interacts with the negatively charged stone silica surface through electrostatic bonds, with the surfactant cation playing a crucial role. This suggests an arrangement where the positive head is oriented towards the stone surface and the non-polar tail upward, explaining the increase in contact angle (Wang and Li, 2020). For Estel treatment, a great increase of the contact angle is detected on both marble and limestone surfaces; behavior ascribable to the residue solvent in the coating. The IL application results in a decrease in the contact angle. The dynamics here may be opposite to those seen with NES+I. The Nano Estel is mostly nonpolar, and when IL is applied, anion and cation are likely oriented with tails downward and polar heads upward. This arrangement enhances the surface's wettability, leading to a low or null contact angle. It is interesting to highlight that the hydrophilicity of the treated surfaces is a characteristic that may contribute to the performance of their antifouling action (Donnelly et al., 2022). TEOS treatment does not change significantly the wettability of the surface of both lithotypes; moreover, IL addition does not affect its behavior. This result aligns with the colorimetric measurements, where the color change after aging is consistent with specimen drying.

Capillary water absorption tests

Capillary absorption tests on treated and aged limestone specimens showed a similar trend in water absorption as the untreated ones (Figure 8).

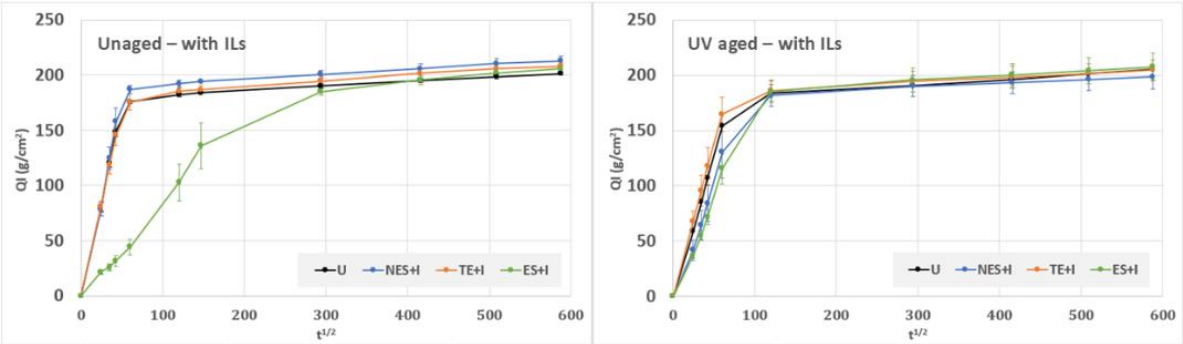

Figure 8. Capillary absorption of untreated, treated and aged limestone specimens.

This was due to the high hydrophilicity acquired by the surfaces according to the results obtained from contact angle measurements. The residual solvent in the Estel coating slowed the capillary water absorption during the first 24 h. Thereafter, the treatment showed the same trend as the other conditions, reaching the saturated state after 5 days from the start of the test. Solvent evaporation that can be induced by UV-daily radiation would explain an acceleration of the process. Through assessment of capillary water absorption on untreated, treated and

aged marble specimens, it was possible to understand the effect of binders and IL on water absorption (Figure 9). Despite marble's low porosity and water uptake, our findings indicate that the treatments have a notable effect. Significant variations in water uptake can be due either to a lower porosity, as pores are filled with the consolidant, or to increased surface hydrophobicity. The behavior of surfaces treated with TEOS and Nano Estel is very similar to that of untreated marble, suggesting that neither condition subsists. In contrast, Estel treatment significantly reduces water absorption.

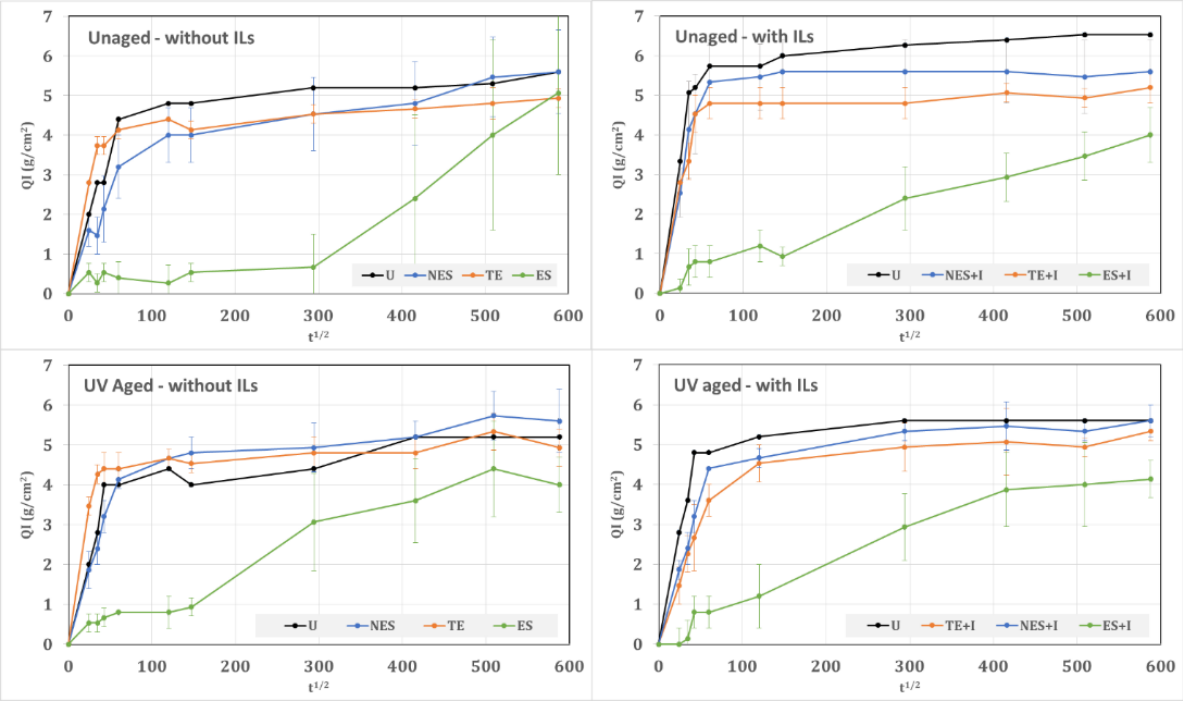

Figure 9. Capillary absorption of untreated, treated and aged marble samples.

This result may be due to temporary hydrophobicity caused by solvent entrapment in the coating during curing, according to colorimetric and contact angle data for the same treatment. Comparing the absorption curves of samples treated with and without IL, we observe that IL slightly affects the Estel binder, resulting in faster water uptake, although the final absorption value remains lower than that of the sample treated with only Estel. The same trend in speeding up of water uptake of Estel-treated/aged limestone specimens is detected for same marble samples. This can be due to solvent evaporation under UV-daylight radiation.

The long-term effects of UV irradiation on the IL mixture alone were evaluated by IR spectroscopy. The spectra obtained from the analysis of IL-treated glass surfaces subjected to UV aging were overlapping (Figure 10). A decrease of water content has been detected by comparing the water OH band centered at 3300 cm-1 and the methyl functional groups

belonging to IL (Figure 11). This is due to continuous exposure to UV irradiation for 507 h at a temperature of about 35 °C.

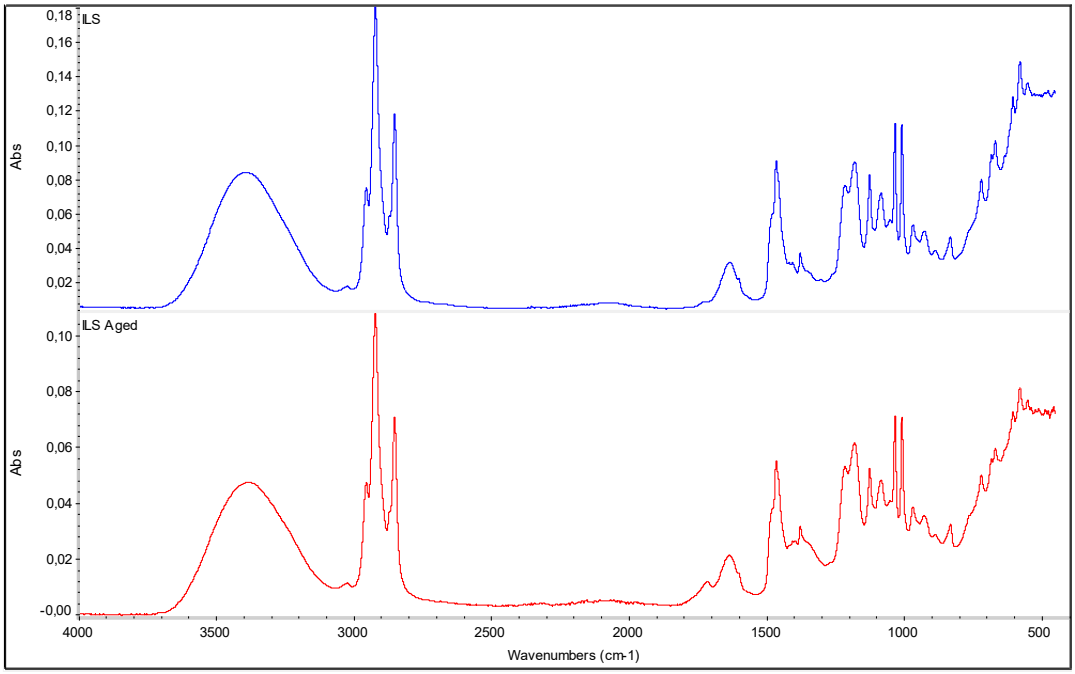

Figure 10. IR spectrum of unaged and aged IL mixture (ILs)

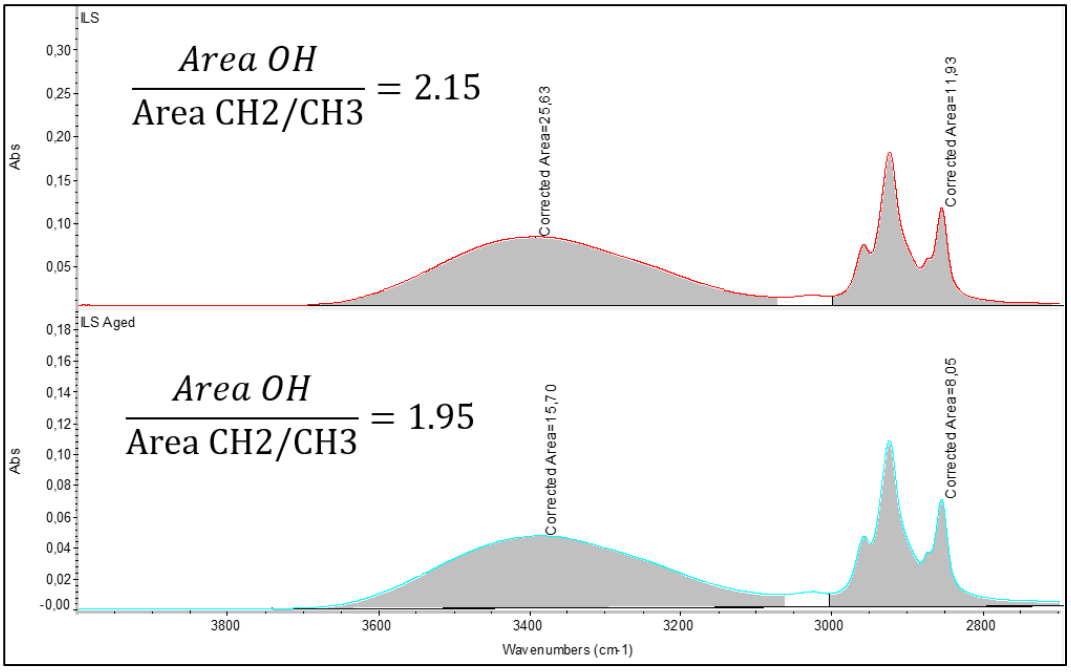

Figure 11. FTIR spectra of IL mixture (ILs) and IL aged. It has been reported the areas of OH and CH_2/CH_3 bands and their ratios.

Laboratory evaluation of coatings durability

Evaluation of erosive action effects exerted by seawater on I-PyrS-treated surfaces showed the durability of coatings applied on marble specimens until the end of the experiment (6 months), was lower when applied on limestone surfaces. In Figure 12 are presented the photos taken on the treated marble and limestone samples with UV radiation, highlighting the luminescence of I - PyrS. Before the test, the blank sample appeared completely devoid of luminescence, and treated samples not yet subjected to washout showed a clearly visible luminescence.

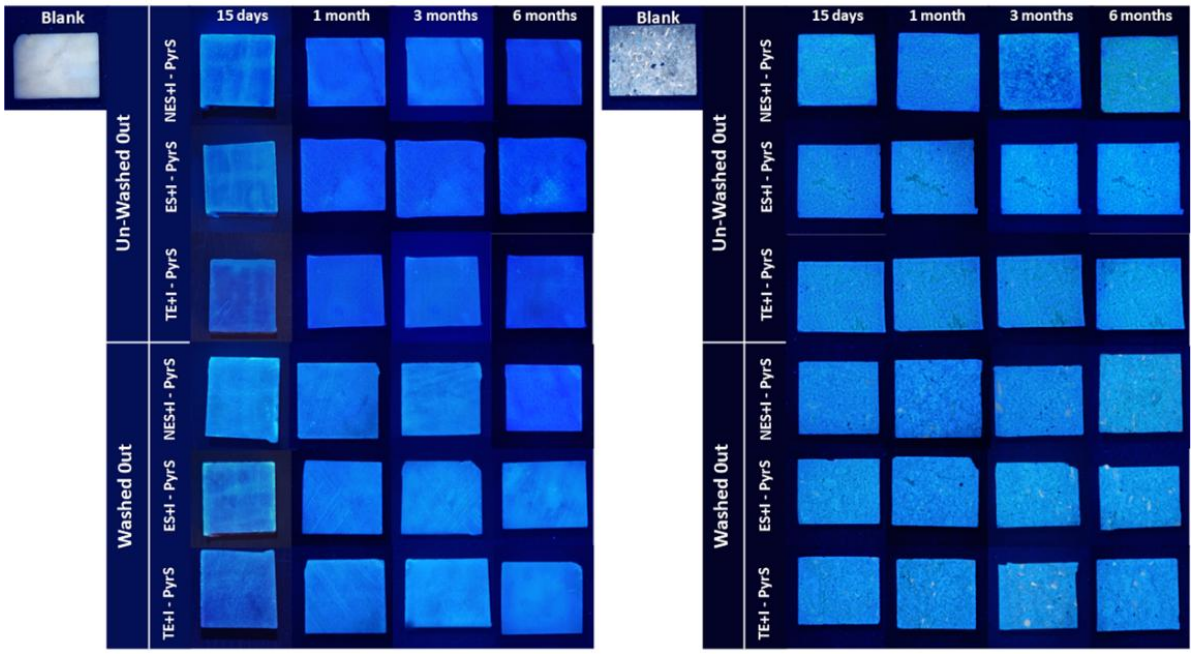

Figure 12. Images of untreated and treated marble specimens un-washed out and washed out up to 6 months on the left and limestone on the right, taken under UV light.

All marble specimens placed in contact with seawater for increasing time intervals showed similar luminescence to unwashed ones. Limestone specimens placed under UV light also show similar luminescence to unwashed ones but, after 3 months, small areas of the I-PyrS-treated limestone surfaces show a loss of luminescence.

As reported in Figure 13, SEM-BSD shows brighter and darker areas that correspond to non-fluorescent and fluorescent areas observed under UV light, respectively. The result is a grayscale image found to be dependent on the surface porosity.

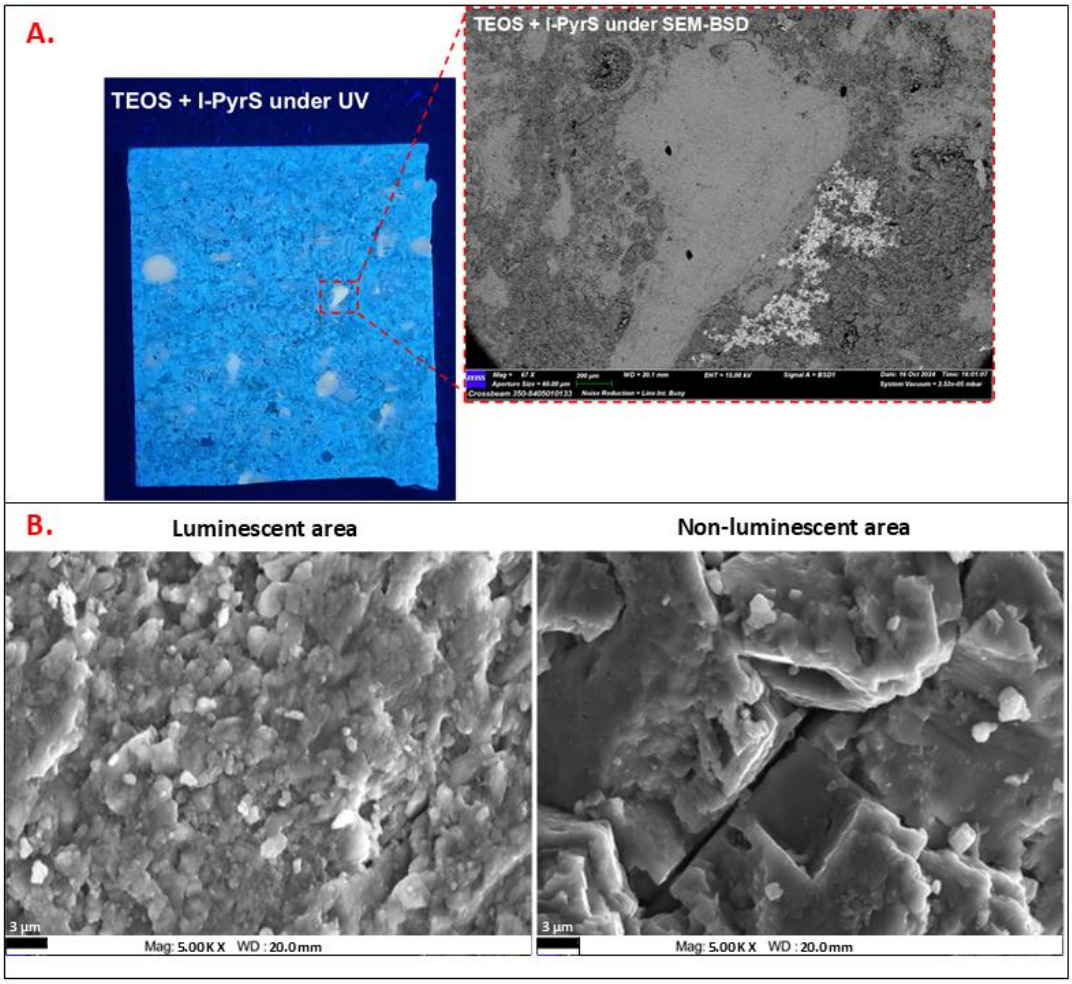

Figure 13. A. Limestone sample treated with tetraethyl orthosilicate plus I-PyrS (TEOS + I-PyrS) and washed out for 3 months, observed under UV light and SEB-BSD; **B.** SEM images of the luminescent and non-luminescent areas of treated limestone surfaces washed-out for 3 months.

The coating applied to a stone surface is absorbed by capillarity. When the coating is applied to an uneven calcareous surface, the coating strips from the compact areas to the porous areas. Following application, even the most compact areas exhibit a thin layer of coating, resulting in a homogeneous luminescent limestone surface, as demonstrated by the unwashed-out samples. Competitive absorption between porous and more compact areas does not occur on marble surfaces. Marble specimens have the same degree of porosity over the whole surface, allowing homogenous penetration of the coatings. These results agree with those obtained from the microcosm test below.

Figure 14 presents photos taken under UV light of treated marble and limestone samples exposed in the microcosm.

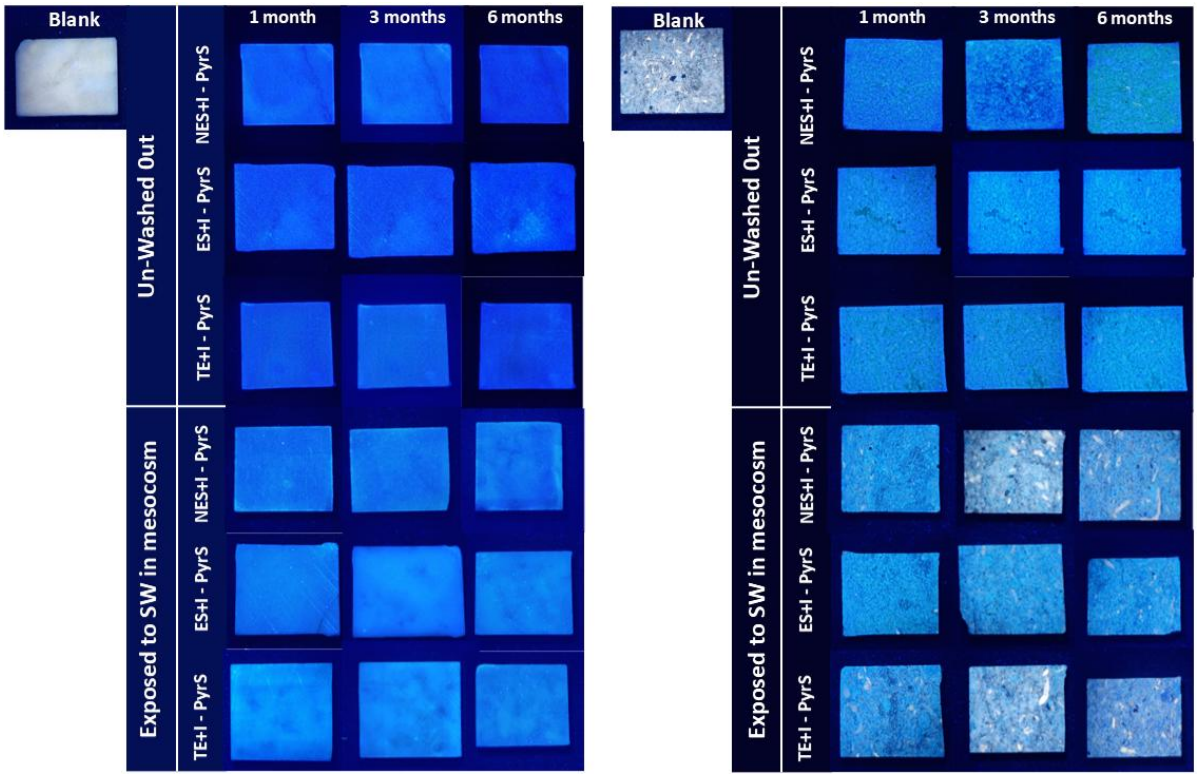

Figure 14. Images of untreated and treated marble specimens un-washed out and exposed to seawater (SW) in mesocosm up to 6 months on the left and limestone on the right, taken under UV light.

All marble specimens sampled at increasing time intervals show a similar luminescence to un-exposed ones, suggesting that IL is resistant for up to 6 months. Unfortunately, it was not possible to continue the experiments to compare these findings to the behavior of probes exposed in the coastal environment that were exposed for a longer period of time (see chapter 2). Limestone specimens placed under UV light also show similar luminescence to un-exposed ones. However, after 3 months from the beginning of the test, small areas of the ES + I-PyrS-treated limestone surfaces show a loss of luminescence; the non-luminescent spots are clearly visible on the samples treated with NES + I-PyrS and TE + I-PyrS. The compactness present in some areas of the surface does not allow capillary absorption of coatings, which is almost completely lost over time.

CONCLUSIONS

The combination of IL with the consolidants/binders Nano Estel, TEOS, and Estel 1000, used as adhesion promoters on marble and limestone surfaces, seems to have a negligible impact on the surface aspect but a significant effect on the wettability of both lithotypes. Limestone surfaces characterized by high porosity keep a high degree of wettability even after treatment. In contrast, the monolayer treatment containing IL (TE+I) had no effect on the wettability of marble surfaces. However, the addition of IL significantly increased the hydrophilicity of marble treated with bilayer coatings (NES+I, ES+I) compared to untreated ones. The hydrophilicity nature of treated surfaces may contribute to their antifouling performance *in situ*. Water molecules on hydrophilic surfaces can give rise to a hydration layer that inhibits the settlement of microorganisms (Donnelly et al., 2022). In addition, coatings applied on marble surfaces demonstrated resistance to both UV radiation and the erosive action exerted by seawater until the end of the experiment (6 months). Having verified the applicability of the coatings on stone surfaces and their mid-term durability, the use of the engineered coating in the underwater contexts can reasonably be considered a viable option.

CHAPTER 2

PERFORMANCE OF THE STONE PROBES IN MARINE ENVIRONMENT

INTRODUCTION

The colonization of stone surfaces by biofoulers poses a major challenge to the preservation of underwater cultural heritage (UCH). The settlement of these organisms and their interactions result in surface deterioration, biofilm formation and encrustations that cause irreversible damage (Crisci et al., 2010; Flemming et al., 2016; Muhammad et al., 2020). Understanding the dynamics of interaction between biofoulers and inorganic stone materials is crucial for developing effective, long-term conservation strategies. However, despite the relevance of this topic, there is still a lack of comprehensive studies investigating how these interactions occur *in situ* within marine environments. This knowledge gap hinders the development of targeted solutions for protecting submerged stone artifacts. In particular, research on antifouling coatings specifically designed for underwater cultural heritage is still in embryonic stage. Continued exploration of biodeterioration mechanisms and material-biofoulers interactions remains essential to identify more sustainable and efficient protective strategies. The present chapter aims to contribute in this context and investigate the effects of inorganic surface treatments with eco-friendly antifouling coatings based on *ILs of third generation* as already successfully reported in previous studies in terrestrial environment by Lo Schiavo et al., 2020; De Leo et al., 2021 and Alì et al., in prep. Further, antifouling tests of IL were carried out in a semi-dry environment. The coating was applied to an area of the marble lunette of the Falconieri fountain located in the historic centre of Messina, Italy. Tetraethyl orthosilicate was used as a consolidant/binder for IL and after 5 years after application, spontaneous colonization was strongly reduced. The next challenge was testing the possible use in submerged environment. The present studies focus on evaluating how different consolidants/binders can improve IL bonding and *in situ* durability when applied to underwater stone surfaces.

MATERIALS AND METHODS

Design of the experimental set

Cage preparation and probes placements

In order to perform underwater experiments, the untreated and treated marble and limestone specimens were cut into 2.5 × 2.5 × 2 cm^3 and treated as described in chapter 1. Blocks consisting of four probes held together with two plastic ties were then made (Figure 15B). The blocks were placed inside a marine steel cage of dimension 90 × 60 × 50 cm^3, organized according to 3 tiers where each sampling time was placed in independent tiers (Figure 15A). Moreover, control blocks (U/NES/TE/ES) were placed in the external part of the cage, while those containing IL-treated specimens (U/NES+I/TE+I/ES+I) were put in the internal part (Figure 15B), to have representativity of the whole area contained in the cage. Plastic ties were used to bind the blocks vertically between two polypropylene tubes located in the cage, avoiding contact with each other and leaving free surfaces exposed to seawater.

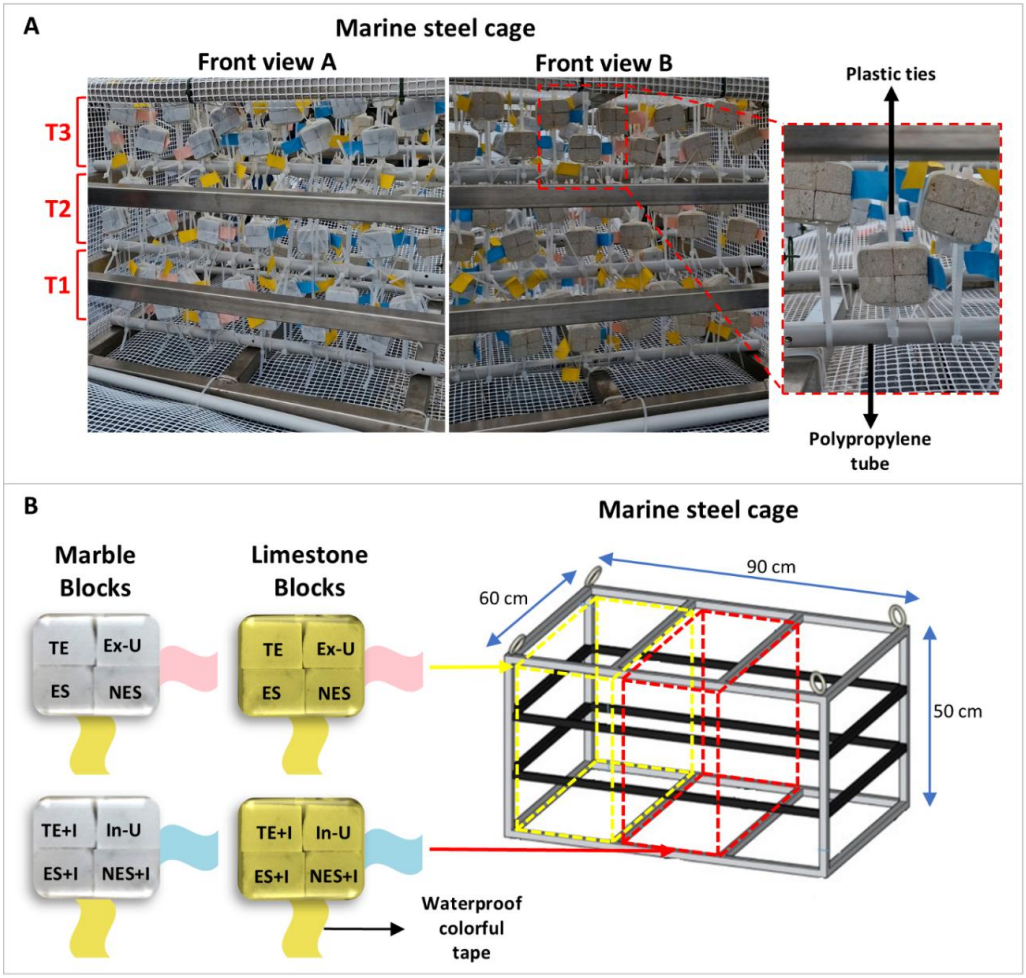

Figure 15. Schematization of experimental set. **A.** Blocks of four specimens held together with two plastic ties fixed vertically between two polypropylene tubes placed inside the marine steel cage. Front view A

marble blocks, front view B limestone blocks, organized on three tiers according to sampling time. **B.** Blocks tagged with waterproof colorful tapes indicating the disposition and treatments included. Yellow dashed cage area, external area where control blocks were placed; red dashed cage area, internal area where blocks containing IL-treated specimens were placed.

Finally, the cage was covered with a net of 5 x 5 mm^2 of mesh size to avoid grazers to access the cage and interfere with fouling process. The cage was located at 200 meters from the Amendolara coastline (Calabria, Italy; coordinates: 39°56'23.04"N 16°36'47.25"E) and at 6 meters depth with 70 cm distance from the seabed and fixed from the bottom through 4 dead bodies and from the top by ropes tied to a big anchor (Figure 16).

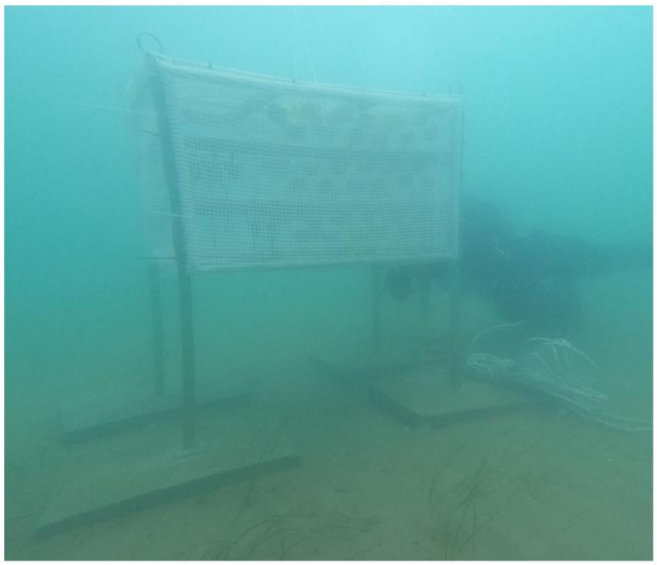

Figure 16. Photo taken during the placement of the marine steel cage at the exposure site on the Ionian coast. © Mirko Mutalipassi

Sampling

Sampling activities (collection of probes, water and sediments) were performed along a time course: 24 hours (T0); 1 month (T1); 6 months (T2); 12 months (T3). For samples taken after 24 hours, the blocks were placed inside a perforated box as in the cage. The perforated box was submerged close to the cage, tied from the bottom to a dead body and from the top to a mooring buoy. Seawater and sediment samples were collected close to the cage at each sampling time. Seawater was sampled using 5 L Niskin bottle and transferred to 2 L sterile bottles previously autoclaved at 121 °C for 20 min. An excess of seawater was taken to fill a large-capacity isothermal container in which the sampled blocks were placed to keep them in a humid environment until processing. Sediments were collected by means of a 5 kg Van Veen grab and transferred into 50 mL sterile falcon tubes (for metabarcoding analysis) and in a 500

mL screw-cap sterile jar (for granulometric analysis). Sediment for granulometry and metabarcoding analysis was stored at + 4 °C and – 80 °C, respectively, while seawater samples were placed at + 4 °C for further filtration and DNA extraction. Marble and limestone blocks were directly processed. Sampled probes, sediments and water were subjected to the following analysis.

Environmental parameters

Environmental parameters were collected close to the cage at each time point: 24 hours, 1, 6 and 12 months from probes exposure. Temperature, salinity and pH was recorded by a multiparametric probe.

Sediments

In order to evaluate the distribution, composition, and texture of sediment samples' particles, they were subjected to granulometric analysis. First, samples were washed twice with bidistilled water and the suspended sediment was allowed to settle at room temperature. Then, supernatant was discarded, and sediments were placed in an oven at + 60 °C for one week. When sediments were completely dry, 500 g was subjected to an initial grain separation with an Agate mortar. Next, sediments were treated with hydrogen peroxide diluted in distilled water in a 2:8 ratio. The samples were left at room temperature and stirred occasionally to facilitate grain separation, and after 48 h, the solution was discarded, and sediments were washed twice with distilled water. After a second drying in the oven, sediment granulometry was performed by means of Digital Sieve Shaker equipped with a series of sieves (2 mm, 1 mm, 500 µm, 250 µm, 125 µm, 63 µm). At the end of the operation, the weight of each fraction was calculated and expressed as a percentage. Based on the obtained grain-size distributions, the percentage of gravel, sand and mud was estimated. The above described process is summarized in Figure 17.

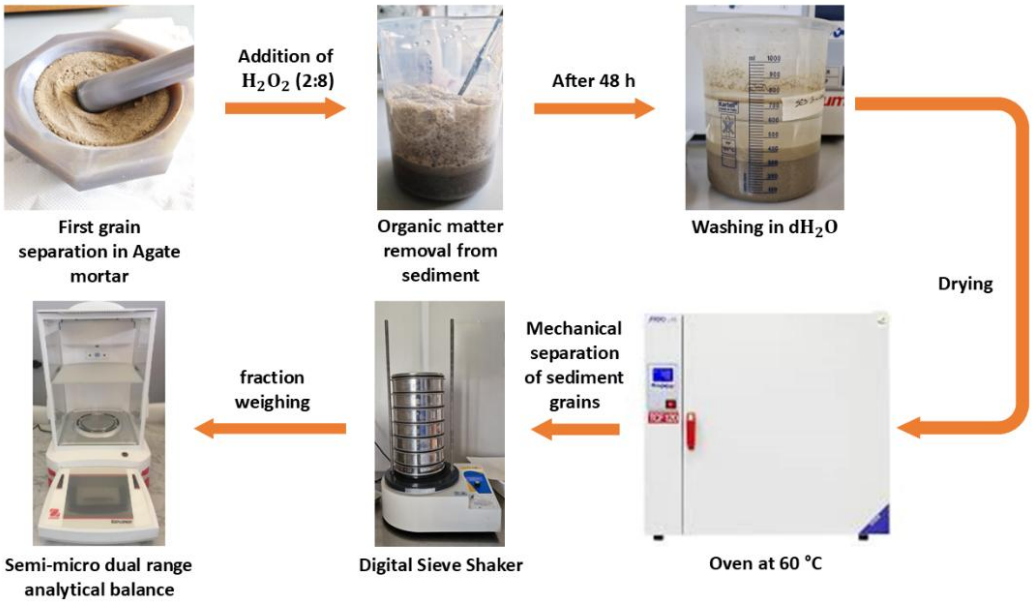

Figure 17. Sediment granulometry process schematization.

Moreover, other sediments sampled close to the cage were subjected to metabarcoding analysis as described in the section *Evaluation of microbial communities of seawater, sediments and colonizing microorganisms through a metabarcoding approach*.

Seawater

Seawater samples were also subjected to metabarcoding analysis. DNA extraction procedures, amplicon sequencing and bioinformatic analysis were reported in section *Evaluation of microbial communities of seawater, sediments and colonizing microorganisms through a metabarcoding approach*.

Probes analysis

Response of treated and untreated probes along the time

To evaluate the fouling response in underwater environment of the treated probes respect the untreated ones along the time (at 24 h, 1, 6 and 12 months), sampled probes were evaluated by different microscopy methods (Stereo, SEM, CLSM) as well as DNA extraction from the sampled probes surfaces and examination through a metabarcoding approach as described below.

- *Stereomicroscopy analysis* of the marble and limestone surfaces untreated and treated with bare binder and binder combined with IL were carried out soon after sampling. For each surface, 3 pictures were taken by means of a Stereoscope Leica S9i with camera and image analysis system at 26 × magnification. The 3 pictures were placed side by side to reconstruct

the whole surface. Combined images were analyzed through ImageJ Software version 1.54p (Schneider et al., 2012) to evaluate the amount of stone surface with high coverage rate exerted by micro- and macro-foulers. Color thresholding (hue and saturation) through iterative self-organizing data (IsoData) algorithm has been performed to divide the image into two classes of pixel corresponding to colored area versus its background. Then, particle analysis has been applied to measure the percentage of pixels (% area) in the selection automatically highlighted by thresholding method. Such percentage values, representing the surface area with high coverage level, have been obtained for each experimental condition and time point.

- *Scanning Electron Microscopy* (SEM) was used to study the degree of biofilm coverage and deterioration of the stone surface. All samples were subjected to fixation in 2.5 % glutaraldehyde and dehydration at increasing ethanol concentrations (30, 50, 70 and 100 %). After total evaporation of alcohol, samples were metallized with graphite and visualized with Ultra-High-Resolution SEM (UHR-SEM) - ZEISS CrossBeam 350 equipment, coupled with the EDS-EDAX OCTANE spectrometer.

- *Confocal Laser Scanning Microscopy* (CLSM) applied at biofilm taken using the adhesive tape sampling method according to previous studies (Urzì and Albertano, 2001; Urzì and De Leo, 2001). Two consecutive samples from each surface were taken to assess the differences between the most superficial colonization and that deeper one (that closer to the stone). Samples on fungi-tape were placed on slides (pre-cleaned with 70 % ethanol) and stored in the dark at + 4 °C until observation. Before visualization, samples were rehydrated with sterile bidistilled water for 30 min at room temperature under solar irradiation. The adhesive tape was then placed on a coverslip (Thermo Fisher, Monza, Italy) of 24 × 60 mm on which a volume of about 90 µL of a solution 0.1 % Acridine Orange AO (Thermo Fisher, Monza, Italy) and bidistilled water was added in a 1:4 ratio. After 10 min of incubation, samples were observed under a confocal microscope (Zeiss LSM 700, Zeiss, Jena, Germany) equipped with argon and helium-neon lasers for excitation of Green Fluorescent Protein (GFP), A488 green and Fluoresceinisothiocyanate (FITC), A594 red. Images were acquired rapidly to avoid photodegradation at 40 × magnification.

Evaluation of microbial communities of seawater, sediments and colonizing microorganisms through a metabarcoding approach

The procaryotic and eukaryotic compositions of biological patinas on stone surfaces, sediments and seawater were characterized through a metabarcoding approach.

DNA extraction

DNA extraction from biofilm and sediment was carried out using the DNeasy PowerSoil Pro Kit (Qiagen, Hilden, Germany) and from seawater samples by DNeasy Power Water kit (Qiagen, Hilden, Germany). The initial extraction procedure described by the manufacturer's protocol was slightly modified, in order to extract DNA from biofilm present on the stone surface. Biofilm was collected by means of a sterile scalpel and resuspended in lysis buffer. Next, the cell lysis phase was carried out in TissueLyser at a frequency of 25 Hz for 10 min. The steps of inhibitor removal, DNA binding, washing and elution were carried out according to the manufacturer's protocol. DNA was extracted from the sediment following the protocol provided by the manufacturer. To extract DNA from seawater, water samples were filtered using a filter funnel attached to a vacuum source, on nitrocellulose membrane of 0.22 µm (2 L for each filter). After addition of lysis buffer on filter membranes, an additional heating step at 65 °C for 10 min was included in the extraction procedure. Homogenization was also performed in TissueLyser (25 Hz, 10 min) followed by centrifugation at 4000 × g for 1 min. The steps of inhibitor removal, DNA binding, washing and elution were then carried out following the manufacturer's protocol. To evaluate DNA integrity, samples were run on 0.8 % agarose gel for 20 min at 80 V using a BIO-RAD horizontal electrophoresis system. A quantitative and qualitative analysis of extracted DNA was carried out with a BioSpec-nano Spectrophotometer (SHIMADZU, Milan, Italy) to obtain the ng/µL concentration and 260/280 and 260/230 ratios. Data variability was quantified by calculating the standard error (se) for each measure, using the formula $se = standard\ deviaton\ /\ \sqrt{n}$, where n represents the number of observations for each measure. Extracted DNA was stored at - 20 °C until shipment for amplification and sequencing.

Amplicon sequencing

Amplicon sequencing from DNA extracted were performed by Bio-Fab Research (Rome, Italy). The V3–V4 variable region (~460 bp) of 16S rRNA and the Eukaryotic V4 variable region (~380 bp) of 18S was amplified following the MiSeq rRNA Amplicon Sequencing protocol (Illumina, San Diego, CA) with some modifications. PCR was performed in a final volume of 25 µL, which was set up with the following quantities: 5 µL of genomic DNA (10 ng/µL in H_2O), 1x PCRBIO HiFi Buffer (PCR BIOSYSTEMS, USA) composed by 1 mM dNTPs and 3 mM $MgCl_2$, 0.5 units of PCRBIO HiFi Polymerase (PCR BIOSYSTEMS, USA) and 0.2 µM of each primer. Cycling conditions followed an initial denaturation at 95 °C for 3 min, 25 cycles of 95 °C (30 s), 55 °C (30 s), 72 °C (30 s), final extension at 72 °C for 5 min, hold at 4 °C. DNA amplicons were cleaned up by MagSi-NGSPREP Plus beads (Euroclone, Milan, IT) and Illumina Nextera adaptor-primers were then used to barcode each sample through PCR as follows: 5 µL of cleaned up DNA amplicon, 1x PCRBIO HiFi Buffer (PCR BIOSYSTEMS, USA) composed by 1 mM dNTPs and 3 mM $MgCl_2$, 0.5 units of PCRBIO HiFi Polymerase (PCR BIOSYSTEMS, USA) and 0.2 µM of each primer; cycling conditions followed an initial denaturation at 95 °C for 3 min, 8 cycles of 95 °C (30 s), 55 °C (30 s), 72 °C (30 s), final extension at 72 °C for 5 min, hold at 4 °C. DNA amplicons were cleaned up by MagSi-NGSPREP Plus beads (Euroclone, Milan, IT) and final library was quantified by QuDye dsDNA HS Kit (Lumiprobe, Hannover, DE). Samples were pooled and sequenced on an Illumina MiSeq™ platform according to the manufacturer's specifications to generate paired-end reads of 300 base-length.

Bioinformatic analysis

Bioinformatic analysis was performed thanks to the genetics, molecular microbiology and bioinformatics (GMMB) research group at the CHIBIOFARAM Department of the University of Messina (Italy). Raw sequencing data were processed with FastP software (version 0.20) to remove adapter sequences and low-quality reads (Sliding Window 4 with mean Phred-score: ≤ 20) (Chen et al., 2018). Paired-end data were then merged using PEAR software (Zhang et al., 2014). Data were imported into QIIME2 (version 2024.5) (Bolyen et al., 2019) using the SingleEndFastqManifestPhred33V2 format, followed by the amplicon sequence variant (ASVs) feature table construction and denoising using the DADA2 pipeline (Callahan et al., 2016) with default settings. High-quality sequences were taxonomically classified with the feature-classifier classify-sklearn command using a pre-trained classifier based on SILVA

database (release 138.1). Microbial community data were processed using R (Version 4.4.1) and RStudio (R Core Team, 2024). Necessary packages such as ggplot2 (Wickham, 2016), dplyr (Wickham H et al., 2023) and vegan (Oksanen J et al., 2025) were loaded to facilitate the analysis on structured text files including sample metadata and operational taxonomic unit (OTU) tables. Taxonomic abundance data were normalized using total sum scaling to account for differences in sequencing depth among samples. Pielou's evenness was calculated to assess ecological diversity. These diversity measures were applied to normalized abundance data, providing the basis for comparison across different conditions and replicates and visualized to compare microbial evenness across conditions. Multivariate linear models were fitted to the data using MaAsLin2 (Mallick et al., 2021), a bioinformatics tool for discovering associations between microbial communities and environmental or experimental conditions. This involved adjusting for multiple comparisons, enhancing the reliability of identified associations between microbial taxa and experimental conditions. Graphically, the averaged values of relative abundances were plotted, cutting off values below 3.5 %.

RESULTS AND DISCUSSIONS

Environmental parameters

The environmental parameters, temperature, salinity and pH, collected at each time point follow seasonal dynamics remaining quite constant over time (Table 2).

Table 2. Environmental parameters collected by a multiparametric probe after 24 hours, 1, 6 and 12 months from the start of stone specimen exposure (T0, T1, T2 and T3, respectively).

PARAMETERS	TO	T1	T2	T3
Temperature (°C)	16.8	16.8	17.3	17.1
pH	8.21	8.19	8.09	8.16
Salinity (psu)	38.6	38.7	38.4	38.8

Sediments

The sediment granulometry at each sampling time showed a greater representation of the sand fraction. At the sampling conducted after 1 day, 1, 6 and 12 months (T0, T1, T2 and T3 respectively), the sediment at the exposure site consisted mainly of sand. Sand represented on average 90 % of the sediments sampled at T0, T1 and T2 (91.6 % at T0; 89.5 % at T1 and T2), the value increased in the last time sampling (T3) to 97 % when mud represented only 3 % of the sediment sample (Figure 18). The sediment grain size never reached more than 2 mm (Gravel = 0).

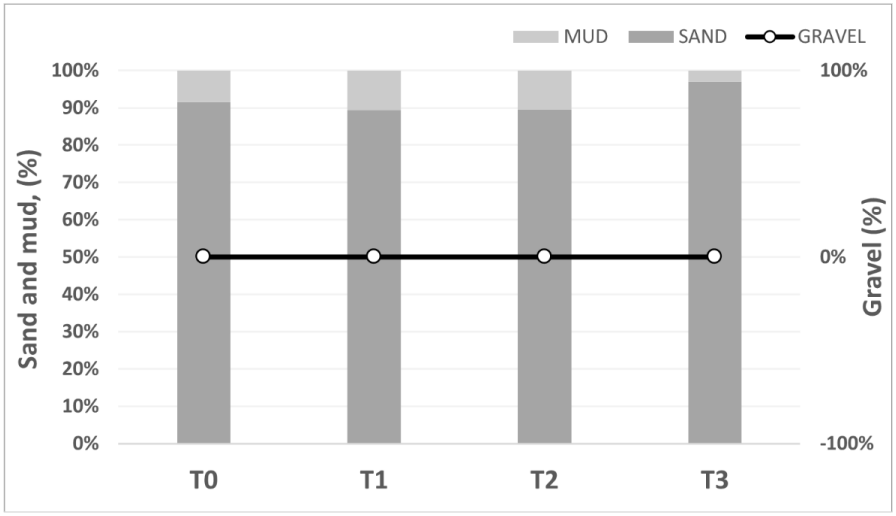

Figure 18. Granulometric measurements of sediment samples collected *in situ* after exposure of probes to the marine environment for 24 h, 1, 6 and 12 months (T0, T1, T2 and T3, respectively).

The physical properties of sediments influence the settlement of microorganisms and the accumulation of organic matter (Zheng et al., 2014). Unfortunately, bioinformatic analysis of sediment samples are in progress, but the literature reports that sand content can provide a suitable substrate for the growth of bacterial phyla such as Cyanobacteria and Actinobacteria (Zheng et al., 2014). Algal domains can establish in a sandy sediment as long as hydrological conditions in the submerged environment make the substrate stable for settlement (Ann et al., 2019).

Seawater

Parameter were reported in Table 2. Metabarcoding analysis performed on seawater close to cage showed the microbial communities of site exposure, potential surface foulers (Figure 19). Seawater samples taken at sampling time 1 month (T1-SW) were characterized by phyla Proteobacteria (26.2 %), Cyanobacteria (43.5 %) and Actinobacteria (30.2 %). At sampling time 6 months (T2-SW) the relative abundance of the phylum Proteobacteria in seawater was considerably increased (69.3 %), while that of the phyla Cyanobacteria (15.6 %) and Actinobacteria (3.7 %) decreased. In addition, a small percentage of relative abundance in T2-SW samples was represented by the phylum Bacteroidota (7.4 %) not present in T1-SW. The relative abundance of the latter increased in seawater samples taken close to the cage exposed for 12 months (T3-SW= 13.4 %) to the detriment of the phylum Actinobacteria (0.1 %). Proteobacteria and Cyanobacteria were also the phyla most prevalent in T3-SW (66.9 % and 15.0 %, respectively).

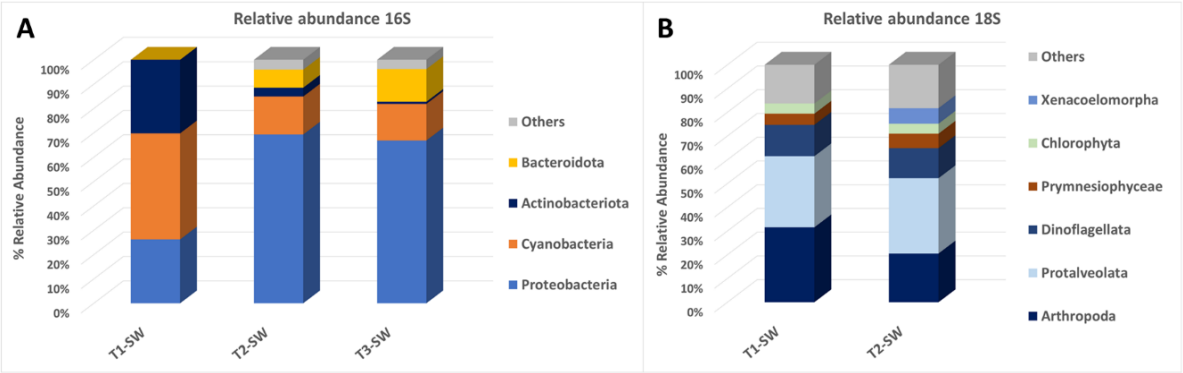

Figure 19. A. Relative abundance of prokaryotic phyla in seawater sampled close to the cage after 1, 6 and 12 months of exposure (T1-SW, T2-SW and T3-SW, respectively). **B.** Relative abundance of eukaryotic phyla in seawater sampled close to the cage after 1 e 6 months of exposure (T1-SW and T2-SW, respectively).

18S Metabarcoding showed the eukaryotic community present in seawater samples. The phyla Arthropoda, Protalveolata and Dinoflagellata represented most of the relative abundance of the communities in the seawater close to the cage exposed for 1 and 6 months (T1-SW and T2-SW, respectively). At T1 sampling time, the phylum Arthropoda had a relative abundance of 32 %, followed by Protalveolata (30 %) and Dinoflagellata (13.2 %). Remaining relative abundance was characterized by phyla Prymnesiophyceae (4.7 %) and Chlorophyta (4.3 %). The relative abundances of the phyla were almost overlapping with those obtained for T2-SW, with the addition of 6 % of the phylum Xenacoelomorpha.

It was not considered useful to carry out metabarcoding analysis of seawater samples taken close to the probes exposed for 1 day as the latter were not found to be colonized. (see the following section *24 hours of exposure (T0)*). 18S metabarcoding of all samples collected at one year of exposure (T3) have been sequenced but, unfortunately, bioinformatic analysis displayed several issues that forced a complete re-elaboration of the data. For this reason, results obtained at this time point were not reported in the present thesis.

Fouling response of treated and untreated probes along the time

In the following sections, the binder control (NES, ES and TE) and ILs-treated (NES+I, ES+I and TE+I) specimens are discussed side by side with the respective untreated Ex-U and In-U to better argue the effect of the treatments applied to the surfaces. The untreated is not only an experimental control (no treatment) but also a spatial control subject to the same environmental factors as neighboring treated specimens.

Evaluation through Stereo- and Scanning electron (SEM) microscopy

24 hours of exposure (T0)

In situ immersion of untreated and treated marble specimens after 24 hours did not allow any evident foulers settlement (Figure 20) confirmed by SEM analysis (Figure 21).

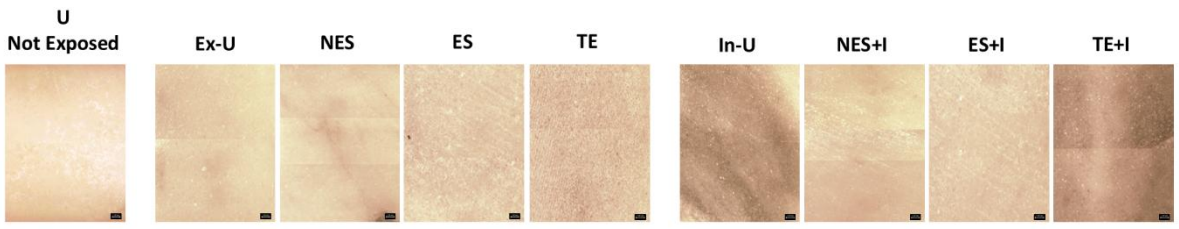

Figure 20. Stereomicroscopy images of untreated and treated marble probes exposed for 24 h, Mag. 26 ×, bar. 1 mm.

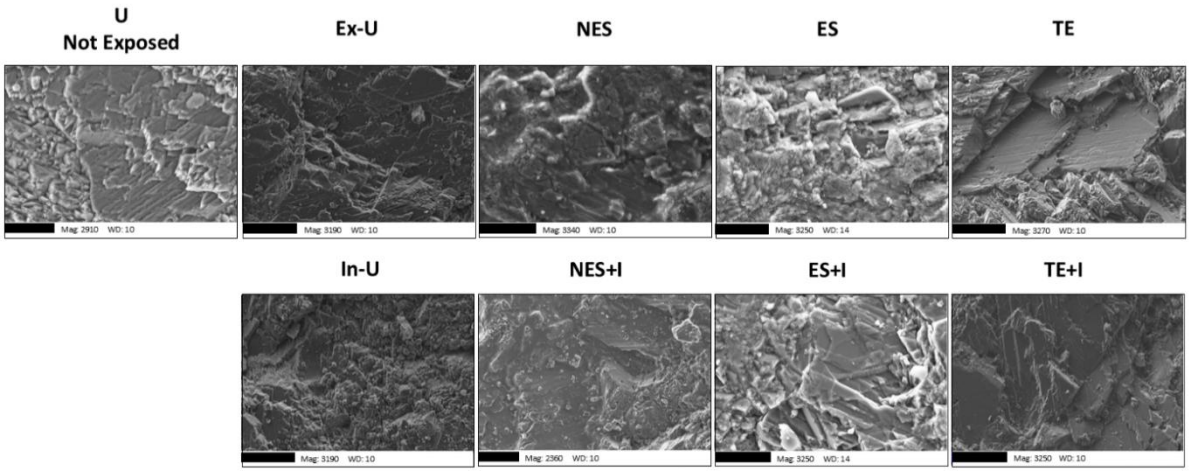

Figure 21. SEM images of untreated and treated marble surfaces exposed for 24 h, bar. 20 µm.

Comparing the untreated surfaces (Ex-U and In-U) and those treated with Nano Estel (NES), a very cracked surface was evident due to the consolidant used. This can be attributed to poor penetration of the nanosilica particles into the stone and the shrinkage that occurs during condensation of the particles. The phenomenon also partially reoccurred on marble surfaces treated with Estel 1000 (ES), where a coating with sporadic cracks was visible. The IL addition never significantly affected the morphology of the coating (Luci et al., 2023). In contrast, surfaces that had been subjected to monolayer treatments with TEOS (TE and TE+I) appeared similar to untreated surfaces, suggesting that the product had penetrated the stone.

Analysis carried out on limestone surfaces also showed the absence of microorganisms after immersion for 24 hours (Figures 22-23).

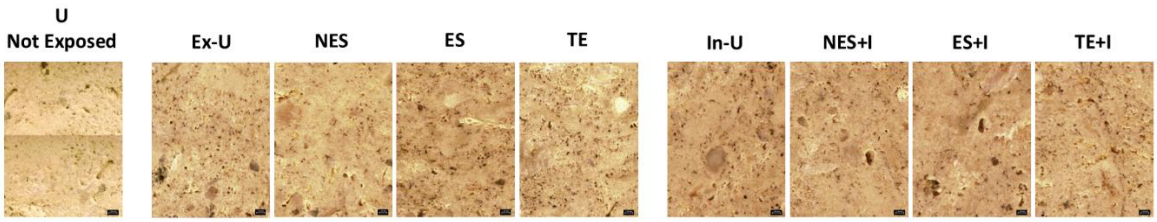

Figure 22. Stereomicroscopy images of untreated and treated limestone probes exposed for 24 h, Mag. 26 ×, bar. 1 mm.

Indeed, limestones appear clean and not biodeteriorated under SEM analysis (Figure 23). Limestone surfaces treated with commercial consolidant Nano Estel (NES and NES+I) only showed a cracked surface. The phenomenon was less evident on limestone surfaces treated with Estel 1000 even than on marble ones, due to the higher surface porosity that allowed better penetration of the consolidant. The limestone surfaces treated with TEOS did not alter

the surface morphology compared to the untreated one, and the addition of IL in each case did not produce variations.

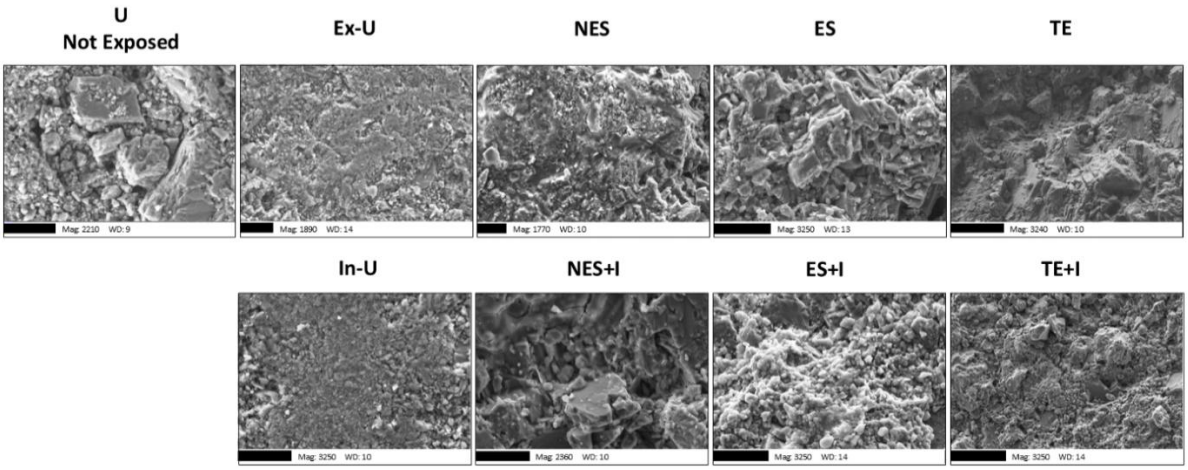

Figure 23. SEM images of untreated and treated limestone surfaces exposed for 24 h, bar. 20 µm.

ImageJ analysis was deemed unnecessary on marble and limestone specimens exposed for 24h without any biofilm coverage.

1 month of exposure (T1)

After 1 month, on the untreated and treated probes, the beginning of the biofouling process is observed. Slight microbial colonization was present on both marble samples exposed in the internal area of the cage and those placed in the external side (Figure 24).

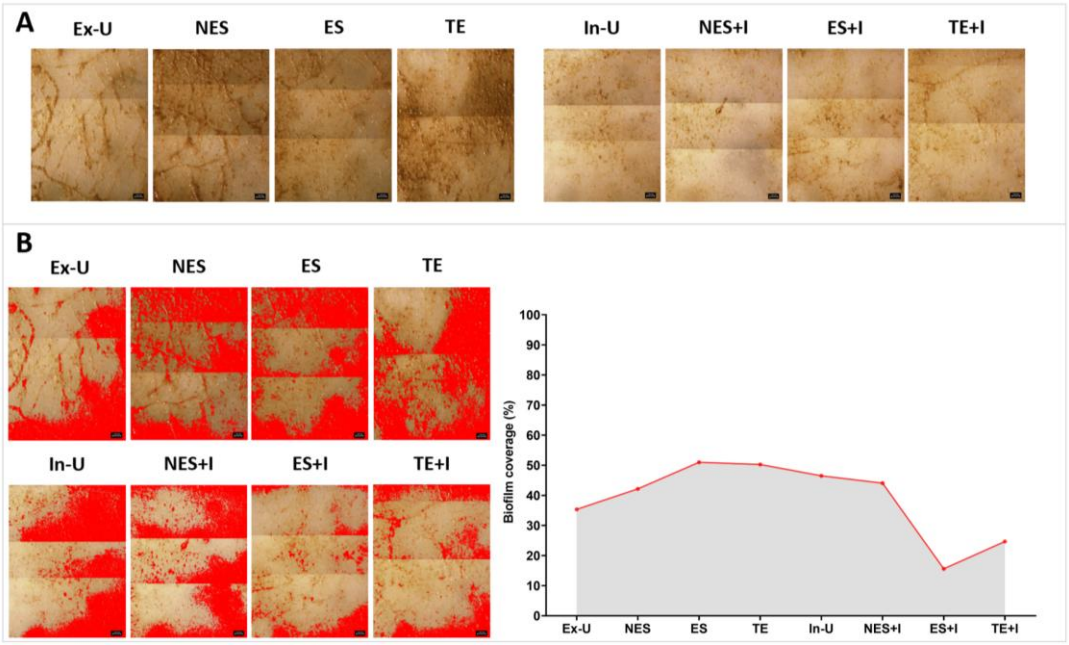

Figure 24. Analysis results of untreated and treated marble probes exposed for 1 month. **A.** Stereomicroscopy images, Mag. 26 ×, bar. 1 mm; **B.** Color thresholding through ImageJ software and percentage of biofilm coverage.

The colonization was influenced by the position in the cage, with the inner samples appearing less colonized in comparison to those placed in the outer side (Figure 24A). ImageJ analysis reported that Estel 1000 and TEOS coupled with IL (ES+IL and TE+IL) were able to contain the fouling process allowing 15.60 % and 24.68 % coverage in comparison to the other conditions reporting higher percentages (>30 %) (Figure 24B).

Microbial colonization of marble surfaces was confirmed by SEM (Figure 25). A greater presence of colonizers embedded in biofilm formations was observed on surfaces not treated with IL, but without evident surface deterioration. The organic fraction of NES+I-treated marble surfaces was slightly higher than that on the other IL-treated surfaces (ES+I, TE+I), as revealed by stereomicroscopy and ImageJ analysis.

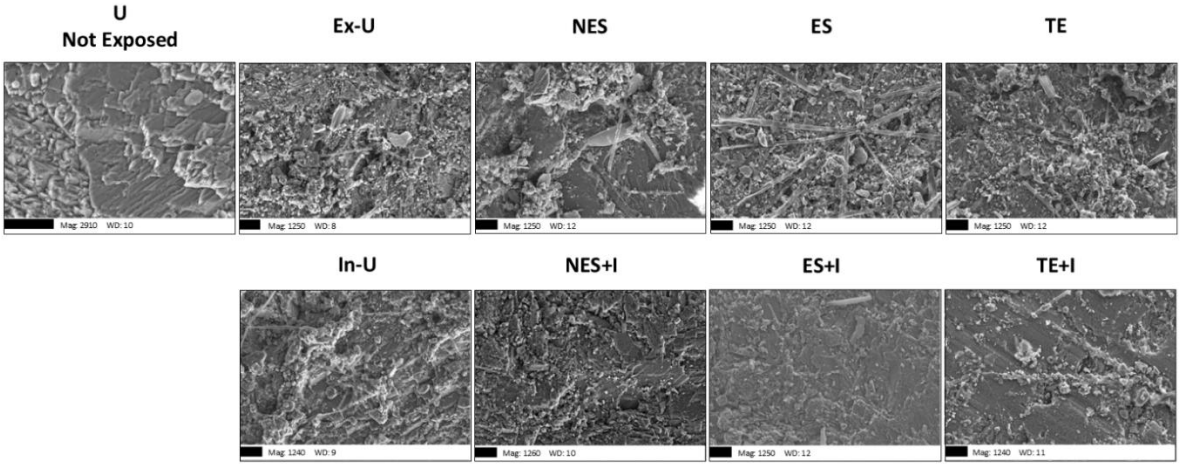

Figure 25. SEM images of untreated and treated marble surfaces exposed for 1 month, bar. 20 μm.

On untreated and treated limestone surface microorganisms were significantly interspersed in the surface pores (Figures 26-27). This was also evinced from ImageJ analysis reporting an increasing amount of micro- and macro-foulers in all experimental conditions, although a certain mitigation in TEOS, Estel 1000 and Estel 1000 + IL has been observed (~32-36 %) (Figure 26B).

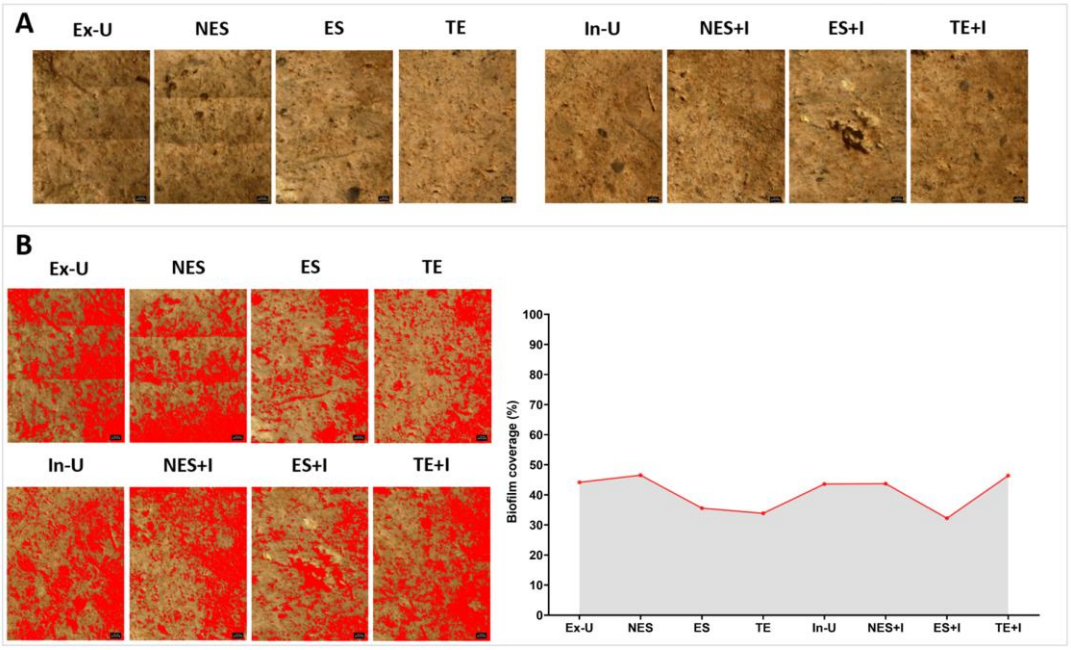

Figure 26. Analysis results of untreated and treated limestone probes exposed for 1 month. **A.** Stereomicroscopy images, Mag. 26 ×, bar. 1 mm; **B.** Color thresholding through ImageJ software and percentage of biofilm coverage.

Microorganisms, located mainly within the pores, were also observed by SEM, but there was no evidence of surface deterioration (Figure 27). Unfortunately, no significant differences could be appreciated between untreated and treated surfaces nor between those treated with the different coatings tested.

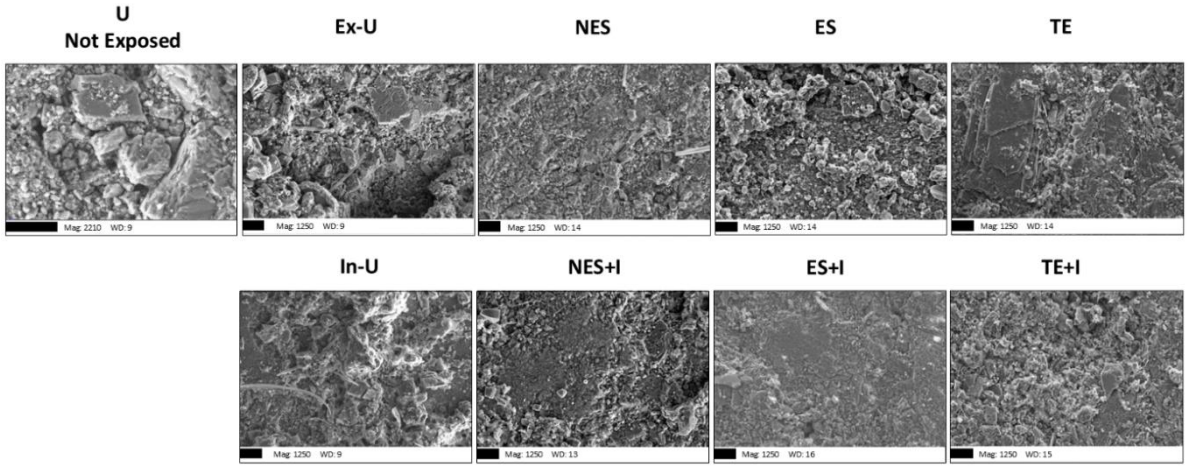

Figure 27. SEM images of untreated and treated limestone surfaces exposed for 1 month, bar. 20 µm.

6 months of exposure (T2)

After 6 months of exposure, limestone surfaces appeared more deteriorated than marbles, probably due to micro- and macro-organisms penetrating inside the stone layer. (Figures 28A-30A). All treatments applied on marble surfaces didn't limit the growing of micro- and macro-foulers since the percentage of covered area measured by ImageJ software exceeded the 40%, except NES samples (36 %) (Figure 28B).

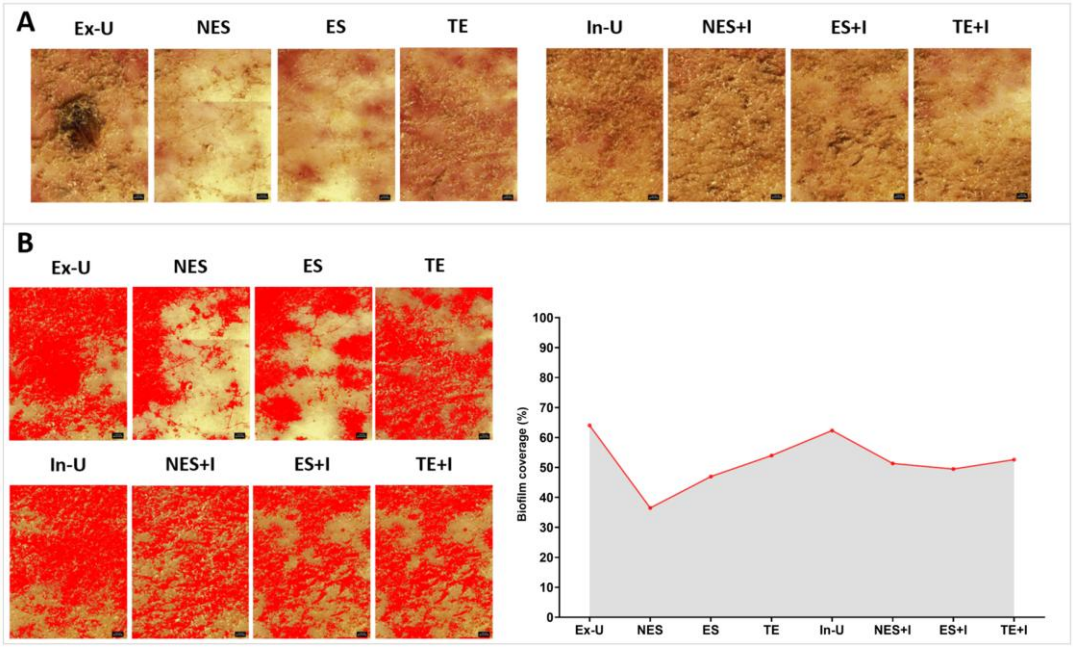

Figure 28. Analysis results of untreated and treated marble probes exposed for 6 months. **A.** Stereomicroscopy images, Mag. 26 ×, bar. 1 mm; **B.** Color thresholding through ImageJ software and percentage of biofilm coverage.

SEM images showed organic coverage regardless of treatment with no appreciable differences between the conditions tested (Figure 29).

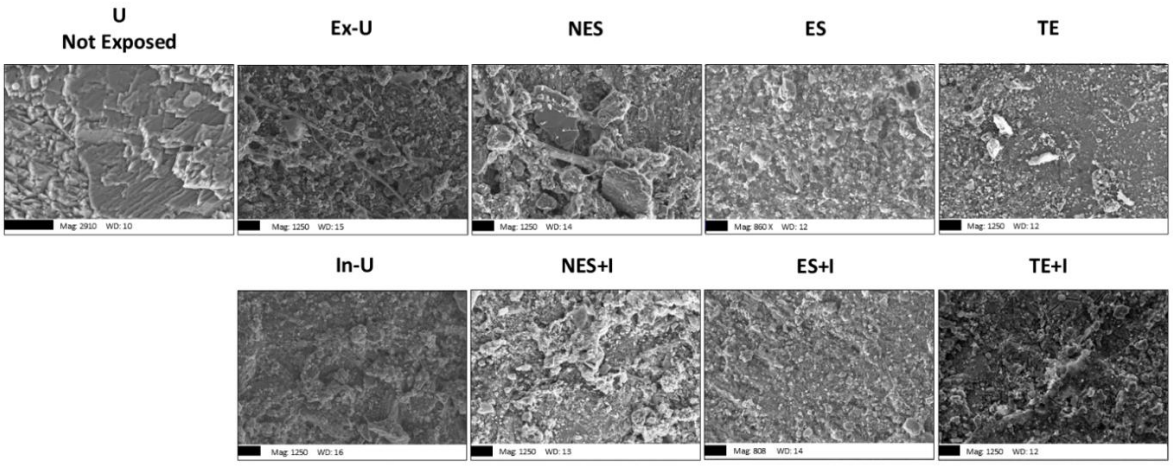

Figure 29. SEM images of untreated and treated marble surfaces exposed for 6 months, bar. 20 µm.

Limestone probes sampled after 6 months of exposure showed a considerable biofouling displayed under stereomicroscopy and confirmed by ImageJ analysis (Figure 30). The latter reported high coverage rate with percentages greater than 50 % in all experimental conditions (Figure 30B).

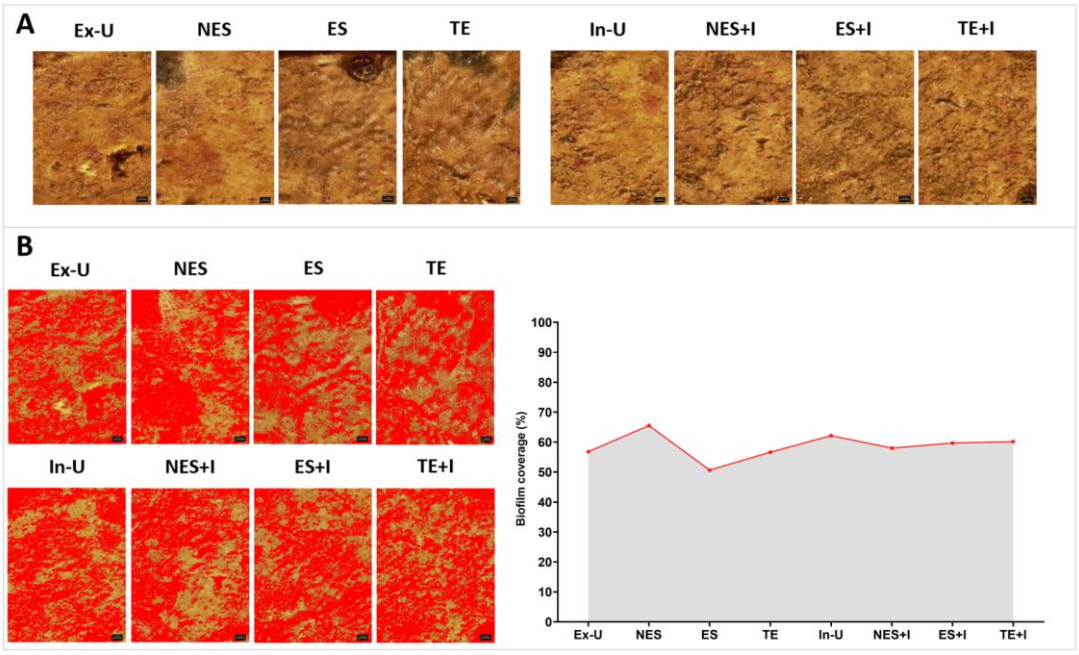

Figure 30. Analysis results of untreated and treated limestone probes exposed for 6 months. **A.** Stereomicroscopy images, Mag. 26 ×, bar. 1 mm; **B.** Color thresholding through ImageJ software and percentage of biofilm coverage.

As marble surfaces, SEM images of limestones exposed for 6 months exhibit organic coverage regardless of treatment (Figure 31). However, untreated samples placed in the inner part of the cage (In-U) showed traces of deterioration by pitting, undetected on IL-treated conditions.

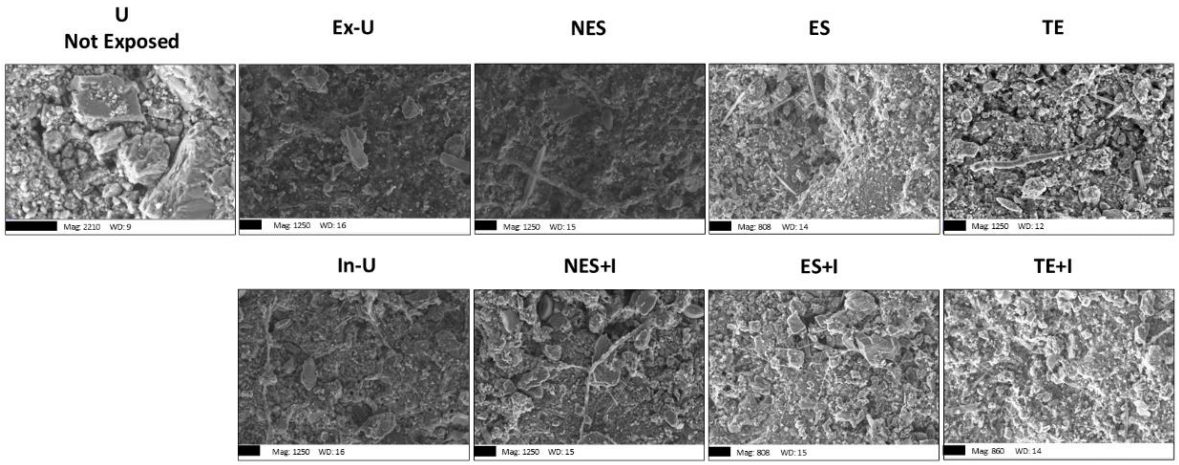

Figure 31. SEM images of untreated and treated limestone surfaces exposed for 6 months, bar. 20 µm.

12 months of exposure (T3)

Marble and limestone surface exposed to marine environment for 12 months suffered serious biodeterioration (Figures 32A-34A). ImageJ analysis reported high coverage rate in all marble conditions, with highest values observed in samples located in external part of the cage (Ex-U= 66.11 %; NES= 75.07 %; ES= 69.24 %; TE= 74.37 %). Interestingly, the untreated samples exposed in the internal part of the cage (In-U) showed a slightly higher coverage than Ex-U, nevertheless, IL addition limited the percentage of micro- and macrofoulers (In-U= 69.31 %; NES+I= 47.92 %; ES+I= 51.70; TE+I= 58.06 %) (Figure 32B).

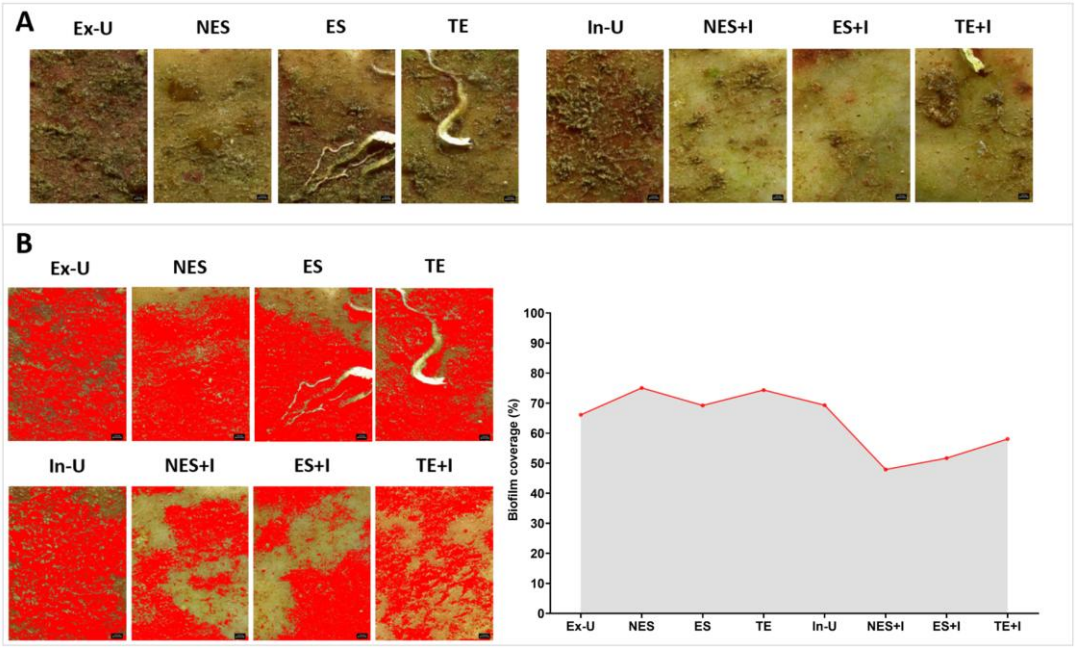

Figure 32. Analysis results of untreated and treated marble probes exposed for 12 months. **A.** Stereomicroscopy images, Mag. 26 ×, bar. 1 mm; **B.** Color thresholding through ImageJ software and percentage of biofilm coverage.

According to the above results, the marble surfaces appeared to have been protected by the coating containing IL applied in two steps under SEM investigations (Figure 33).

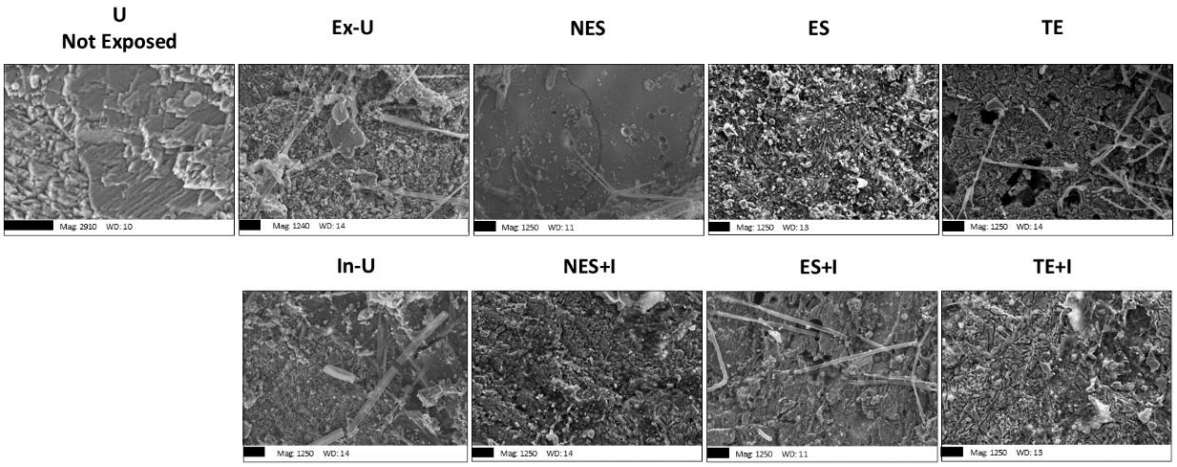

Figure 33. SEM images of untreated and treated marble surfaces exposed for 12 months, bar. 20 μm.

The NES marble surfaces showed thick biofilm coverage, and the TE and ES marble surfaces showed grooves assimilated to the action of biofoulers as on the untreated (Ex-U, In-U) and TE+I surfaces. The NES+I and ES+I marble surfaces had significantly less deterioration despite the settlement of microorganisms.

After one year of exposure, the limestone surfaces appeared to be widely colonized. ImageJ analysis confirmed this considerable degree of coverage with high percentage of covered area that reached values of ~ 78% in the untreated samples located in the internal part of the cage (In-U) (Figure 34B). However, it was evident that the coverage differed between untreated and treated specimens and between specimens treated with bare consolidant and with IL-added consolidants (Figure 34A).

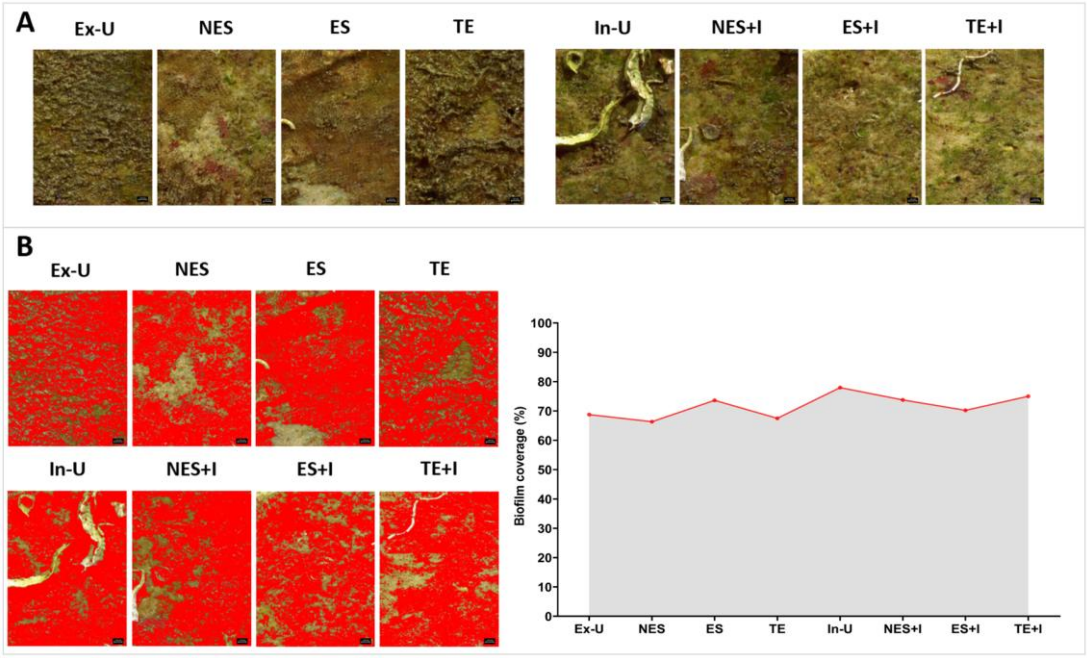

Figure 34. Analysis results of untreated and treated limestone probes exposed for 12 months. **A.** Stereomicroscopy images, Mag. 26 ×, bar. 1 mm; **B.** Color thresholding through ImageJ software and percentage of biofilm coverage.

The variation was apparently dependent on the position of the specimens within the cage as the surfaces of the untreated specimens Ex-U and In-U also differed under SEM analysis (Figure 35). The limestone surfaces NES, ES, and TE showed a thick organic coverage that was structurally different from each other and fully covers the stone substrate. IL-treated surfaces appeared under SEM with a less structured but homogeneous organic coverage that caused surface deterioration.

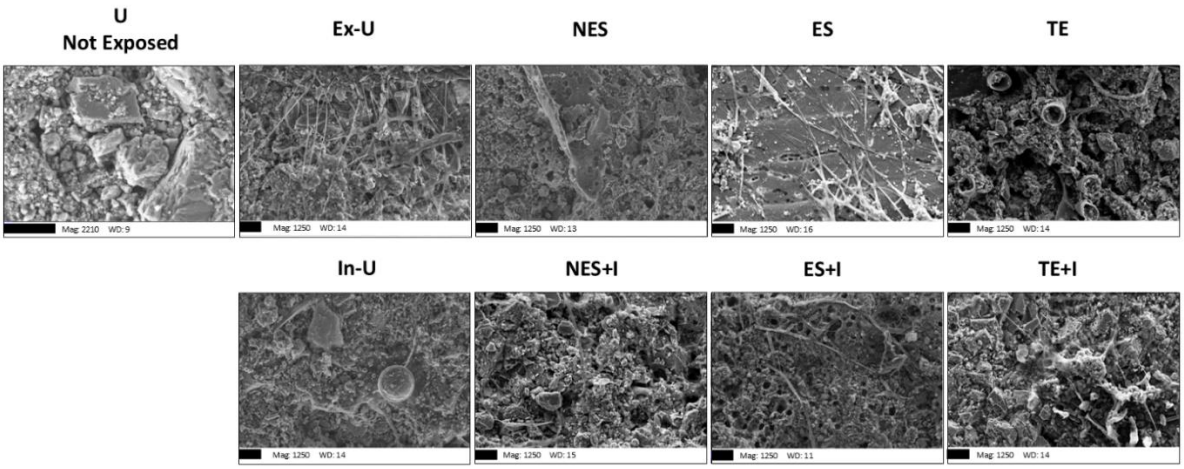

Figure 35. SEM images of untreated and treated limestone surfaces exposed for 12 months, bar. 20 µm.

Stereomicroscopy and SEM observations demonstrated different pattern of colonization depending on the lithotype and position in the cage.

Evaluation through Confocal Laser Scanning microscopy and Metabarcoding

The combination of CLSM observations and metabarcoding, evidenced the main responsible of the fouling that took place on submerged stone surfaces. CLSM analysis of the most superficial layer and the layer closest to the marble surface showed that biodeterioration in the marine environment is implemented by both bacteria and microalgae, as also confirmed by the metabarcoding results of the 16S and 18S rRNA regions. Untreated and treated marble and limestone surfaces exposed *in situ* for 24 h showed no degree of biodeterioration under stereomicroscopy and SEM analysis. For this reason, results obtained only at T1, T2 and T3 time points were reported below.

1 months of exposure (T1)

Confocal microscopy analysis of the untreated marble surfaces exposed for 1 month (T1-U) showed a thick biofilm layer characterized by the presence of bacteria responsible for biofilm production and the empty spaces were perfectly colonized by microalgae (Figure 36). A similar biofilm coverage was observed on the TEOS-treated surfaces (T1-TE), with a first layer mostly characterized by microalgae. The presence of the consolidants Nano Estel and Estel 1000, on the other hand, favored the microbial clusters of about 300 μm in size. On T1-ES, clusters were rich in microalgae and bacteria, but the bacteria were significantly lower on T1-NES. With the addition of IL, the biofilm coverage appeared more rarefied. Significantly smaller microbial clusters and less bacteria were evident on samples treated with Estel 1000 combined with IL (T1-ES+I).

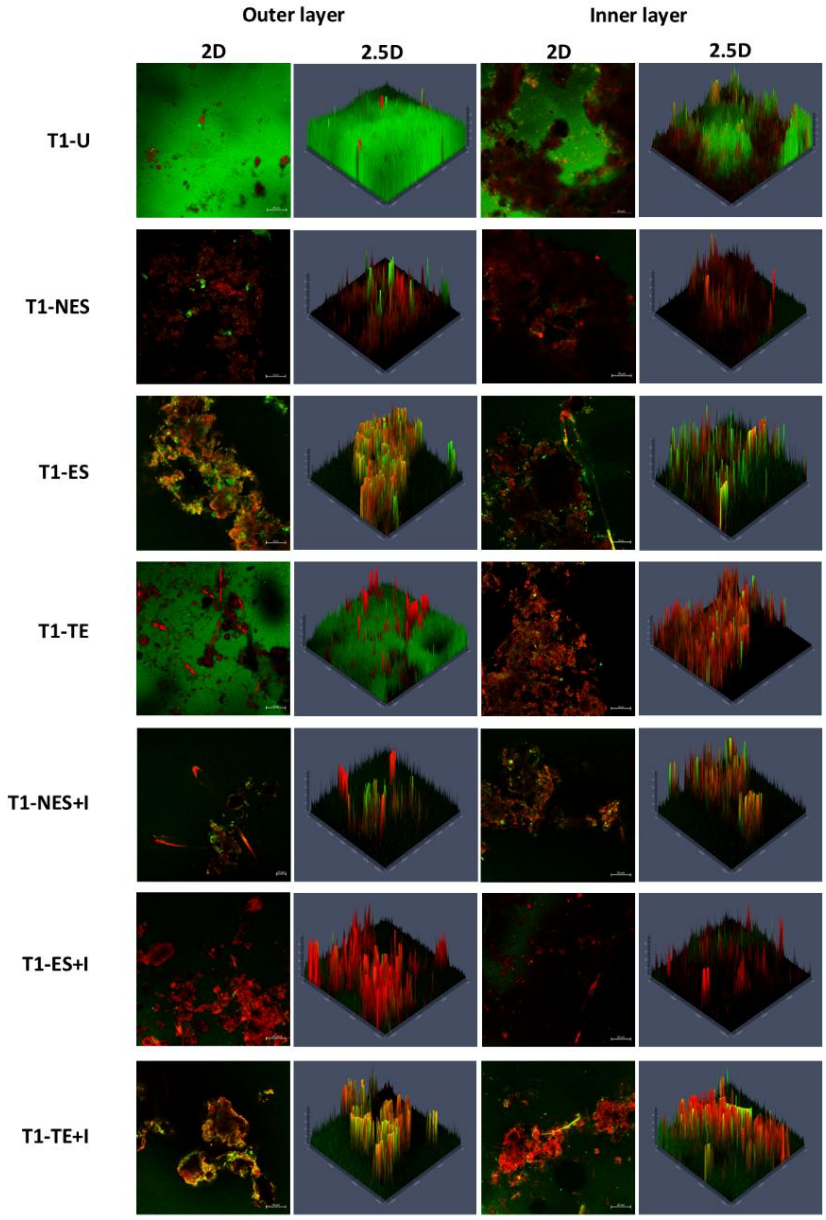

Figure 36. 2D and 2.5D CLSM images marble specimens exposed for 1 month *in situ*; algae colored in red and bacteria in green, bar. 20 µm.

Metabarcoding analysis of DNA extracted from the specimens' surfaces placed at different areas in the cage (reported in metabarcoding graphs as “In” for internal samples and “Ex” for external ones) demonstrates the actual biological variability among the tested conditions responsible for different biofouling processes (Figure 37). After 1 month, 16S Metabarcoding analysis reported predominance of Proteobacteria and Cyanobacteria phyla on all surfaces (Figure 37A). In addition, the phyla Planctomycetota and Bacteroidota were found on the surfaces but not in seawater.

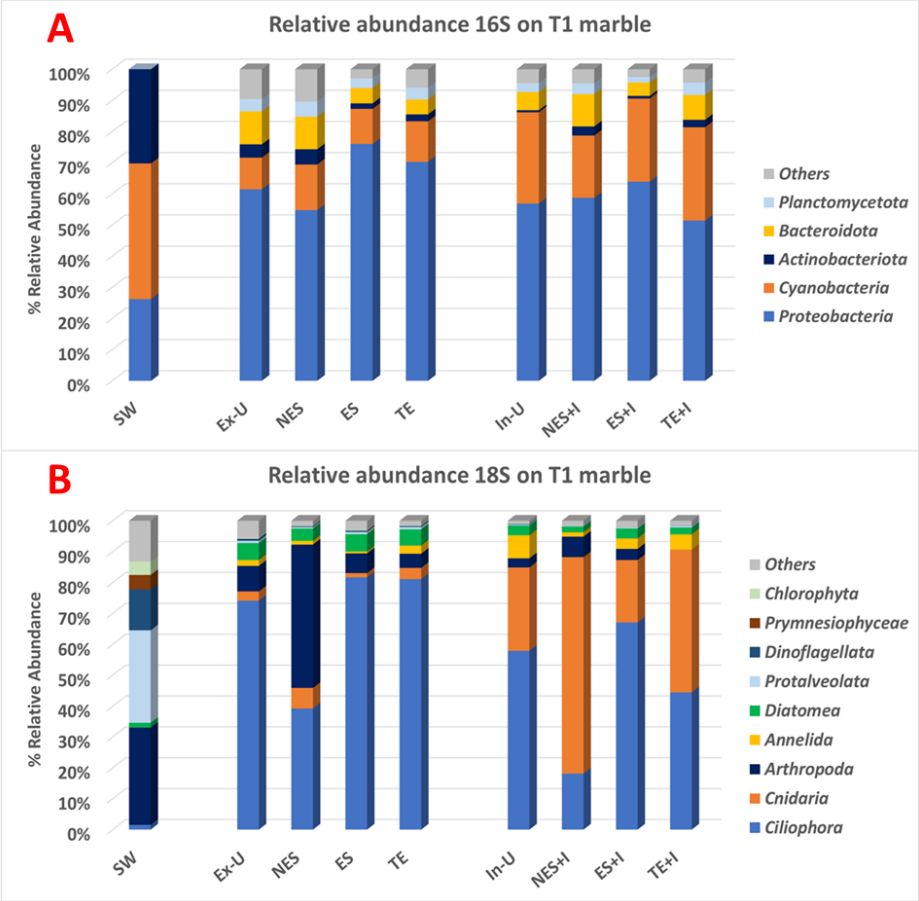

Figure 37. Metabarcoding results obtained from marble specimens exposed for 1 month *in situ*. **A.** Relative abundance of procaryotic phyla; **B.** Relative abundance of eucaryotic phyla.

Proteobacteria represented on average 73 % of the relative prokaryotic abundance found on marble surfaces treated with TEOS and Estel 1000 (TE= 70.3 %; ES= 76.0 %). Its relative abundance decreased by 18 % on surfaces treated with Nano Estel alone (54.7 %), resulting in lower even than the untreated sample (61.4 %) and favoring the settlement of the phylum Bacteroidota (10.4 % on NES, 4.9% on ES, 4.8 % on TE), behaving as the untreated sample (Ex-U= 10.6 %). In the internal area of the cage, where the IL-treated specimens and the corresponding untreated control (In-U) were present, the same phyla settled on the surfaces. The relative abundance of Proteobacteria on the untreated and IL-treated surfaces was comparable to that of the untreated specimen placed in the external part of the cage (In-U= 56.9 %, NES+I= 58.9 %; ES+I= 63.9 %; TE+I= 51.4 %). However, the relative abundance of the phylum Cyanobacteria increased (Ex-U= 10.2 %; In-U= 29.3 %; NES+I= 20.0 %; ES+I= 26.7 %; TE+I= 30.0 %). This variation could be attributed to the different position within the cage, but the decrease in the relative abundance of the phylum Proteobacteria on ES+I and

TE+I, could solely depend on the presence of IL. In addition, the amount of DNA extracted from the untreated surface located in the internal area of the cage was appeared to be higher than that extracted on the specimens exposed in the external area, and the DNA extracted from the IL-treated surfaces lower than that collected from the In-U control (Table 3).

Table 3. BioSpec-nano quantification of DNA extracted from marble surfaces exposed for 1 month *in situ* and targeted for sequencing of 16S and 18S regions.

SAMPLING TIME	SURFACE	CND	CONCENTRATION (ng/cm^2)	*se*
T1	Marble	Ex-U	0.34	0.71
		NES	1.02	0.49
		ES	0.59	0.19
		TE	0.83	0.06
		In-U	3.42	1.47
		NES+I	1.10	0.45
		ES+I	0.66	0.25
		TE+I	1.48	0.76

Regarding eukaryotes (Figure 37B), Ciliophora is the phylum with the highest relative abundance on all marble surfaces exposed for one month (58 % on average), but coatings that contain Nano Estel also demonstrated different behavior of marble surfaces compared to the other treatments. The phylum Ciliophora represented only 38 % of the relative abundance found on the NES surface compared to 79 % found on the other conditions Ex-U, ES and TE (74.1 %; 81.6 % and 81.1 %, respectively). However, the percentage of Arthropoda increased on NES (Ex-U= 8.3 %; NES= 46.4 %; ES= 6.2 %; TE= 4.6 %). The trend was comparable to that observed on samples exposed in the internal side of the cage. Ciliophora had a relative abundance of 18 % on NES+I and 58 % on In-U, 67 % on ES+I and 44 % on TE+I. In this case, the decrease of phyla was more appreciable even on the treated surface with monolayer coating (TE+I) giving way to the settlement of phylum Cnidaria (46.2%). Diatoms were ubiquitously present on all marble samples with a relative abundance on average of 4 %.

Since DNA extracted from the limestone surfaces exposed for 1 month was not sufficient for analysis, no data are available at this time point. As observed on SEM images (Figure 27), foulers interspersed within the pores of the limestone surfaces. This did not occur on marble surfaces exposed for 1 month since the porosity was lower. Therefore, the DNA extraction

procedure did not bring to a complete collection of biological patina resulting in a small amount of DNA (Limestone Ex-U 5.3 ng/µl; Limestone In-U 6,7 ng/µl) (Table 4).

Table 4. BioSpec-nano quantification of DNA extracted from limestone surfaces exposed for 1 month *in situ* and targeted for sequencing of 16S and 18S regions.

SAMPLING TIME	SURFACE	CND	ng/µL	*se*	260/280	*se*	260/230	*se*	CONC. (ng/cm^2)	*se*
T1	Limestone	Ex-U	5.30	0.46	1.52	0.04	0.03	0.01	0.18	0.02
		NES	5.57	1.04	1.67	0.15	0.03	0.01	0.19	0.04
		ES	4.20	0.95	1,57	0.17	0.06	0.04	0.14	0.03
		TE	5.43	1.19	1.91	0.25	0.01	0.00	0.18	0.04
		In-U	6.67	0.98	1.68	0.11	0.02	0.01	0.22	0.03
		NES+I	5.00	0.30	1.53	0.09	0.04	0.02	0.25	0.02
		ES+I	4.90	1.20	1.54	0.13	0.26	0.24	0.25	0.06
		TE+I	8.25	1.75	1.66	0.15	0.03	0.02	0.41	0.09

6 months of exposure (T2)

CLSM analysis showed the formation of a thick biofilm layer on untreated (T2-U) and bare consolidant-treated marble surfaces exposed for 6 months *in situ* (Figure 38). On layer closest to the surface of untreated probes a homogeneous biofilm coverage has been detected, while a greater presence of microalgae was observed in the most superficial layer. Less homogeneous biofilm was observed on surfaces treated with Nano Estel and Estel 1000 (T2-NES and T2-ES, respectively), but rich in microbial clusters embedded within it. This explains the differences observed from the stereomicroscopy images (Figure 28). Microbial colonization of IL-treated surfaces was also evident from CLSM images, but microorganisms were responsible for producing a thinner and rarer biofilm, particularly in the case of surfaces treated with the monolayer coating (TE+I).

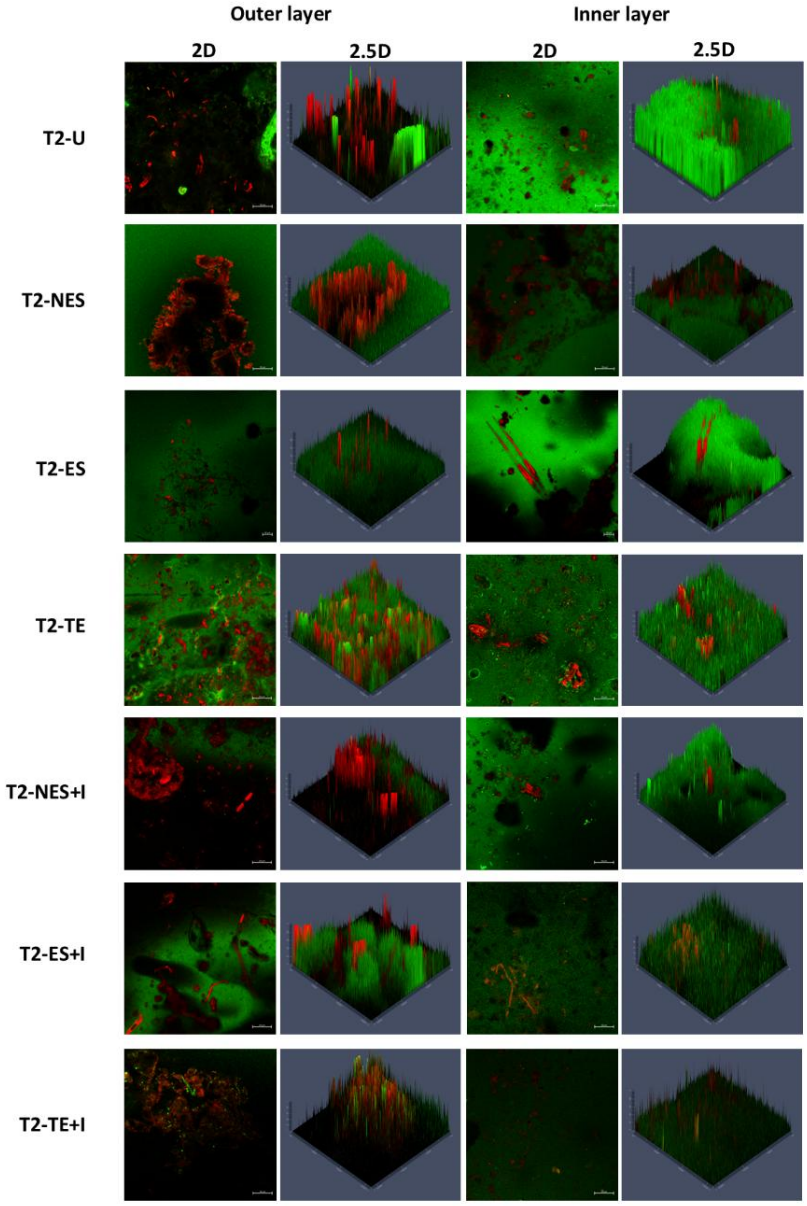

Figure 38. 2D and 2.5D CLSM images marble specimens exposed for 6 months *in situ*; algae colored in red and bacteria in green, bar. 20 µm.

The metabarcoding results showed a reorganization of the phyla present on the surfaces compared to that observed at T1 (Figure 39). In addition, higher biological variability was found in the seawater, but few of these phyla were found on the stone surfaces. Marble surfaces were colonized for 50 % by Verrucomicrobiota (51.4 % on T2-Ex-U; 48.7 % on T2-In-U). Actinobacteria (36.2 %), Planctomycetota (7.8 %) and Cyanobacteria (4.7 %) settled on the untreated specimen placed on the external side of the cage. The inner one, on the other hand, is colonized for the remaining 50 % by Planctomycetota (28.8 %), Proteobacteria (12.8 %) and Actinobacteria (9.8 %). The Nano Estel treated sample behaved like the untreated

sample Ex-U, Verrucomicrobiota, Actinobacteriota, Planctomycetota, and Cyanobacteria were the main phyla recorded on surfaces (47 %, 17 %, 15 %, 21 %, respectively). In contrast, Cyanobacteria were not present on TEOS-treated surfaces; Verrucomicrobiota had a relative abundance of 75 %. The second phylum by relative abundance was Actinobacteriota (25.4 %), which was not present on the Estel 1000-treated surfaces, replaced by Proteobacteria (34.1 %). On specimens placed in the internal area of the cage, the presence of Proteobacteria persisted from T1, but the relative abundance decreased on average to 39 % on untreated sample and NES+I (17.5 %) and to 15 % for TE+I and ES+I (ES+I= 43.2 %; TE+I= 34.0 %). ES+I showed greater biological variability than the other conditions, a significant decrease in the phylum Verrucomicrobiota (NES+I= 48.6 %; ES+I= 7.9 %; TE+I= 33.1 %) but the presence of Cyanobacteria (In-U= 0 %; NES+I= 0 %; ES+I= 12.6 %; TE+I= 1.3 %).

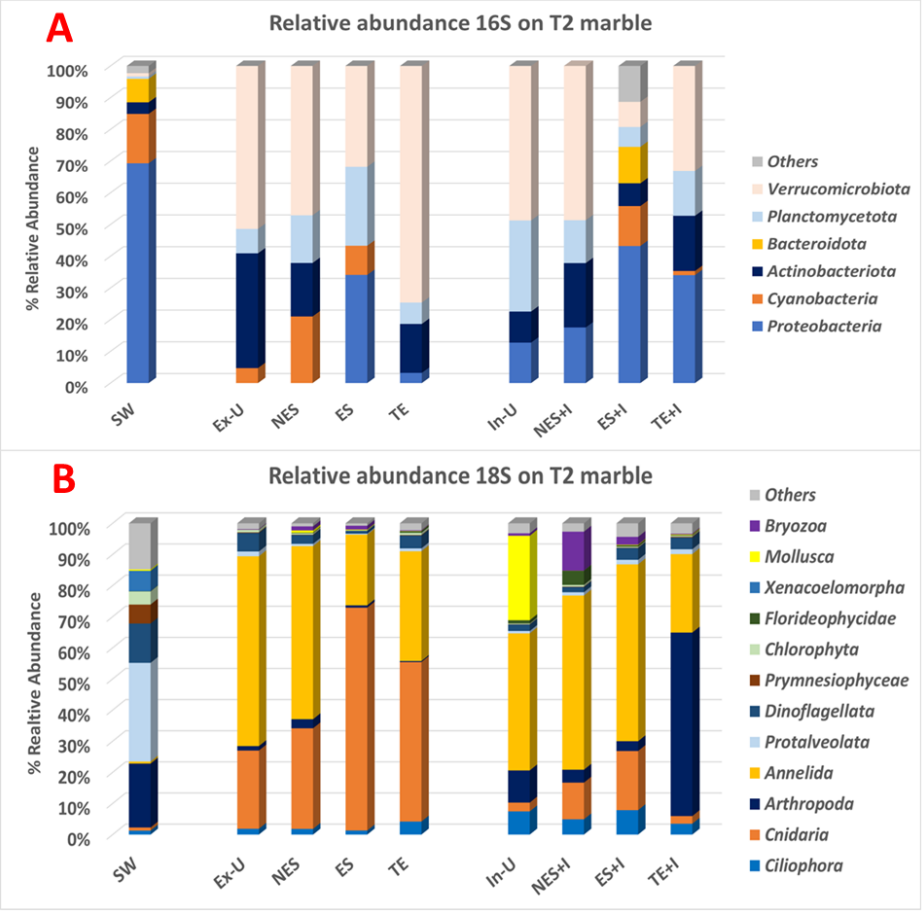

Figure 39. Metabarcoding results obtained from marble specimens exposed for 6 months *in situ*. **A.** Relative abundance of procaryotic phyla; **B.** Relative abundance of eucaryotic phyla.

The eukaryotic phyla settled on the control marble samples placed in the external part of the cage were Cnidaria and Annelida. Cnidaria represented more than 50 % of the relative

abundance found on the specimen treated with Estel 1000 and TEOS (ES= 71.6 %; TE= 51.2 %) and an average of 29 % of Annelida was present (ES= 22.7 %; TE= 35.3 %). On the other hand, untreated and Nano Estel-treated surfaces, reported the phylum Annelida on average of 58 % relative abundance (Ex-U= 61.0 %; NES= 55.6 %). Specimens placed in the internal area of the cage showed a different biological variability from specimens placed in the external side. In the internal area, the relative abundance of Cnidaria decreased (In-U= 2.8 %; NES+I= 11.8 %; ES+I= 19.0 %; TE+I= 2.5 %), whereas the phyla Arthropoda increased (In-U= 10.3 %; NES+I= 4.2 %; ES+I= 3.1%; TE+I= 59.0 %). The phylum Mollusca settled on In-U (27.1 %), but it was not present on the IL-treated specimens; Bryozoa settled more on the latter (In-U= 0.8 %; NES+I= 12.5 %; ES+I= 2.5 %; TE+I= 0.3 %). TE+I is colonized by 59 % Arthropoda at detriment of Annelida (25.2 %). The amount of DNA collected from surfaces treated with consolidants appeared to be slightly higher than that collected from untreated surfaces, and the amount of DNA extracted from the In-U specimen seemed comparable to that obtained from TE+I, potentially indicating higher yields under these conditions compared to others (Table 5).

Table 5. BioSpec-nano quantification of DNA extracted from marble surfaces exposed for 6 months *in situ* and targeted for sequencing of 16S and 18S regions (standard error is not available since we had only one sample).

SAMPLING TIME	SURFACE	CND	CONCENTRATION (ng/cm^2)
T2	Marble	Ex-U	10.99
		NES	12.33
		ES	17.80
		TE	12.43
		In-U	9.30
		NES+I	12.37
		ES+I	11.19
		TE+I	8.08

16S metabarcoding of untreated limestone specimens Ex-U showed presence of only three phyla, 45 % of Proteobacteria, 32 % of Planctomycetota and 23 % Actinobacteria, while that exposed in the internal area (In-U) were colonized by only two phyla Planctomycetota and Actinobacteria (32.4 % and 22.7 %, respectively) (Figure 40A). Limestone specimens treated with Nano Estel and TEOS showed a notable decrease in the phylum Proteobacteria (NES=

7.6 %; TE= 1.2 %) compared to the Ex-U and an increased abundance of Actinobacteriota (NES= 63.5 %; TE= 50.8 %). Its relative abundance increased up to 76 % on surfaces treated with Estel 1000. Planctomycetota was the third phylum to settle on treated specimens NES and TE as well as untreated ones (Ex-U), but its relative abundance decreased on ES-treated surfaces (NES= 27.9 %; ES= 8.8 % TE= 48.0 %). Among the specimens exposed in the internal area of the cage, the sole NES+I surface was colonized by the phylum Proteobacteria (24 %), while the remaining part consisted of Actinobacteriota and Planctomycetota (42.9 % and 33.1 %, respectively), the only two phyla that were found on the other conditions.

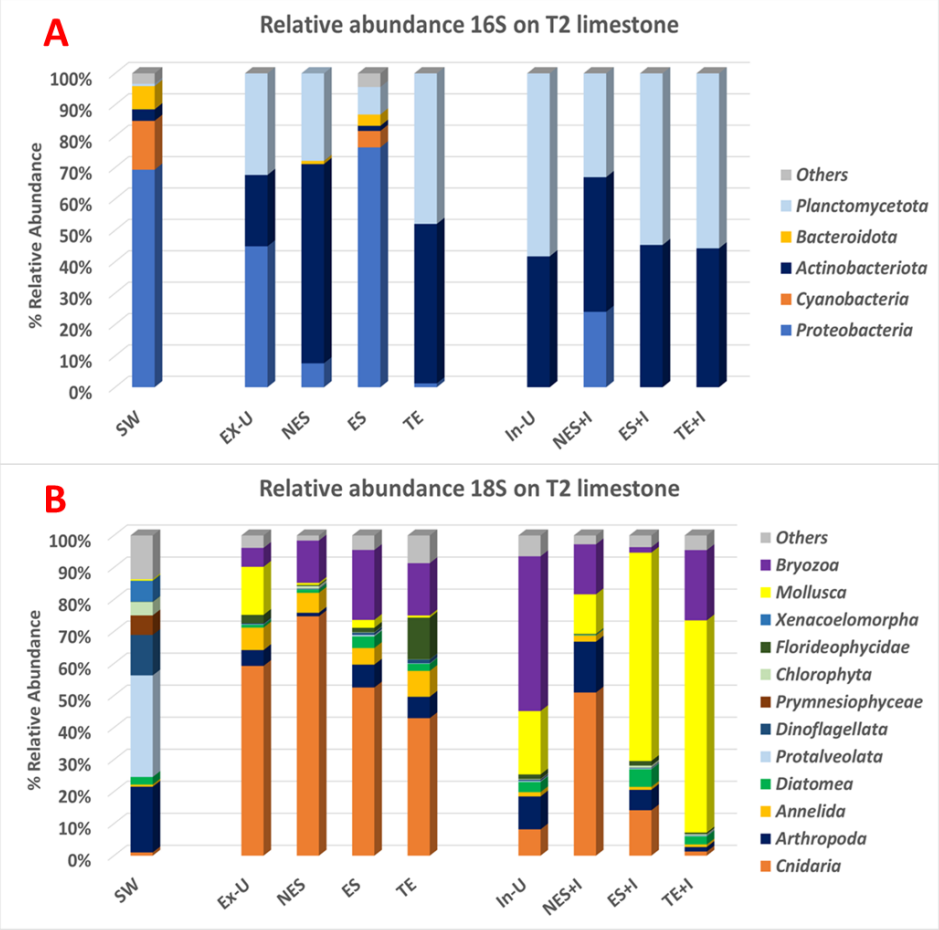

Figure 40. Metabarcoding results obtained from limestone specimens exposed for 6 months *in situ*. **A.** Relative abundance of procaryotic phyla; **B.** Relative abundance of eucaryotic phyla.

On the other hand, the variability of the untreated specimens (In-U, Ex-U) is almost overlapping for eucaryotes (Figure 40B). The phylum Cnidaria had a relative abundance of 59 % on the limestone specimen exposed for 6 months in the external part of the cage (Ex-U), but only 8 % on that placed in the internal part (In-U). In contrast, Mollusca was evenly distributed among the untreated limestone specimens exposed in both area of the cage (Ex-

U= 15.0 %, In-U 19.7 %). The latter phyla decreased on surfaces treated with consolidants (NES= 0.7 %; ES= 2.5 %; TE= 0.7 %), but the phylum Bryozoa increased (Ex-U= 5.9 %; NES= 13.2 %; ES= 21.8 %; TE= 16.3 %), as also confirmed by observations made with stereomicroscopy (Figure 30A). The phylum Cnidaria showed a relative abundance in NES surfaces (75 %) higher than the other conditions (ES= 52.5 %; TE= 42.9 %). The relative abundance of phyla changed considerably on the specimens exposed in the internal area of the cage. The surface treated with Nano Estel + IL was also dominated by Cnidaria (50.9 %), which had a clearly higher relative abundance than the other conditions (In-U= 8.2 %; ES+I= 14.2 %; TE+I= 1.3 %) but lower than the surface not treated with IL (NES= 74.7 %). It should be considered that the percentage of the phylum also decreased on the In-U, so the variation could be attributed to the location within the cage. In addition, it may be worth considering the amount of DNA collected from the surfaces treated with bare Nano Estel and combined with IL, which appears to differ from the other conditions. Before IL treatment, there seemed to be less genetic material than untreated Ex-U and other bare consolidant treatments, whereas after addition of the newly designed coating, the extracted material appeared to be higher in comparison to In-U, ES+I and TE+I (Table 6).

Table 6. BioSpec-nano quantification of DNA extracted from marble surfaces exposed for 6 months *in situ* and targeted for sequencing of 16S and 18S regions (When quantification relies on a single sample, the standard error cannot be computed; the value is therefore reported as NA).

SAMPLING TIME	SURFACE	CND	CONCENTRATION (ng/cm^2)	*se*
T2	**Limestone**	Ex-U	6.54	4.71
		NES	3.14	1.47
		ES	8.44	4.60
		TE	6.10	5.08
		In-U	2.07	NA
		NES+I	4.35	3.65
		ES+I	1.04	NA
		TE+I	0.58	NA

Limestone specimens treated with ES+I and TE+I for 6 months were mainly colonized by the phylum Mollusca (65.1 % and 66.3 %, respectively), with a higher relative abundance than the untreated, replacing the phylum Bryozoa; stereomicroscopy images also showed its almost complete disappearance (Figure 30A). It had a relative abundance of 48 % on untreated

limestone surfaces (In-U), but decreased on IL-treated surfaces, particularly for ES+I (NES+I= 15.6 %; ES+I= 1.7 %; TE+I= 21.9 %).

12 months of exposure (T3)

As seen with SEM, after 1 year of exposure the untreated marble surfaces were covered with a well-structured biofilm (Figure 33), and CLSM images allowed the view of channels built within the biological patina (T3-U, Figure 41). Microalgae were mostly present in the outer layer as at sampling time T2.

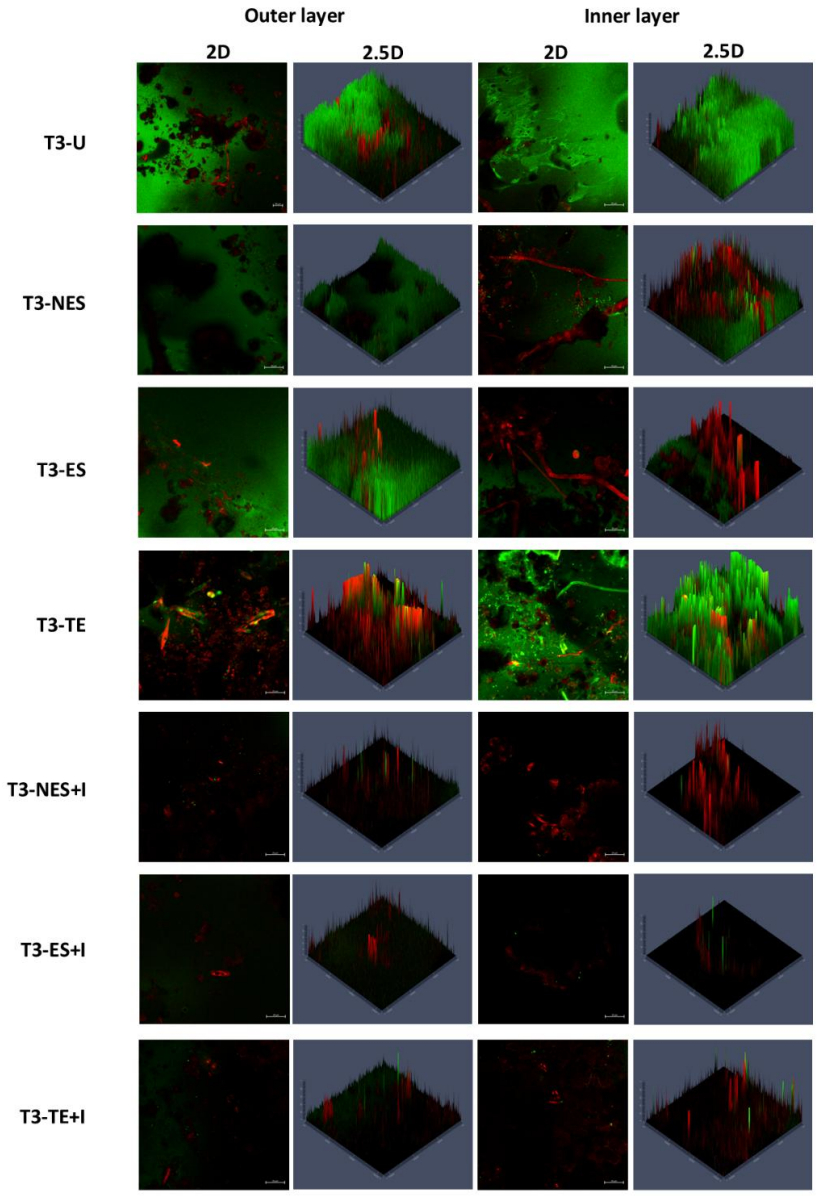

Figure 41. 2D and 2.5D CLSM images marble specimens exposed for 12 months *in situ*; algae colored in red and bacteria in green, bar. 20 µm.

Bacteria and microalgae settled on the surfaces even when treated with bare consolidant and CLSM analysis of treated surfaces witnessed the protective effect of IL (Figure 41). Marble surfaces treated with IL-implemented consolidants showed the almost total absence of biofilm and annexed bacteria, and only small clusters of microalgae were observed. Although the monolayer coating (TE+I) inhibited microbial colonization, it had been unable to protect the stone surface from deterioration in a submerged environment. (Figures 33-41).

The biological variability on marble and limestone surfaces observed by 16S metabarcoding were almost overlapping (Figure 42). Samples taken from the marble lithotype differ from those taken from limestone only in the phylum Planctomycetota not present on the latter where it is replaced by Actinobacteriota. Proteobacteria and Cyanobacteria were the main constituents of microbial community associated to marble and limestone; both phyla formed about 70 % of total microbial community. Their relative abundance on marble samples were on average, 42 % for Proteobacteria (Ex-U= 46.7; NES= 43.0; ES= 41.2; TE= 34.1; In-U= 42.0; NES+I= 39.2; ES+I= 37.6; TE+I= 49.3) and 35 % for Cyanobacteria (Ex-U= 34.1; NES= 29.6; ES= 31.4; TE= 41.8; In-U= 40.1; NES+I= 32.4; ES+I= 35.2; TE+I= 32.7). The amount of DNA collected from the different conditions tested was also comparable (Table 7).

Table 7. BioSpec-nano quantification of DNA extracted from marble surfaces exposed for 12 months *in situ* and targeted for sequencing of 16S and 18S regions.

SAMPLING TIME	SURFACE	CND	CONCENTRATION (ng/cm^2)	*se*
T3	**Marble**	Ex-U	8.46	0.51
		NES	8.82	2.65
		ES	8.28	2.74
		TE	9.26	4.07
		In-U	7.51	1.54
		NES+I	5.75	2.21
		ES+I	9.26	0.18
		TE+I	8.91	1.01

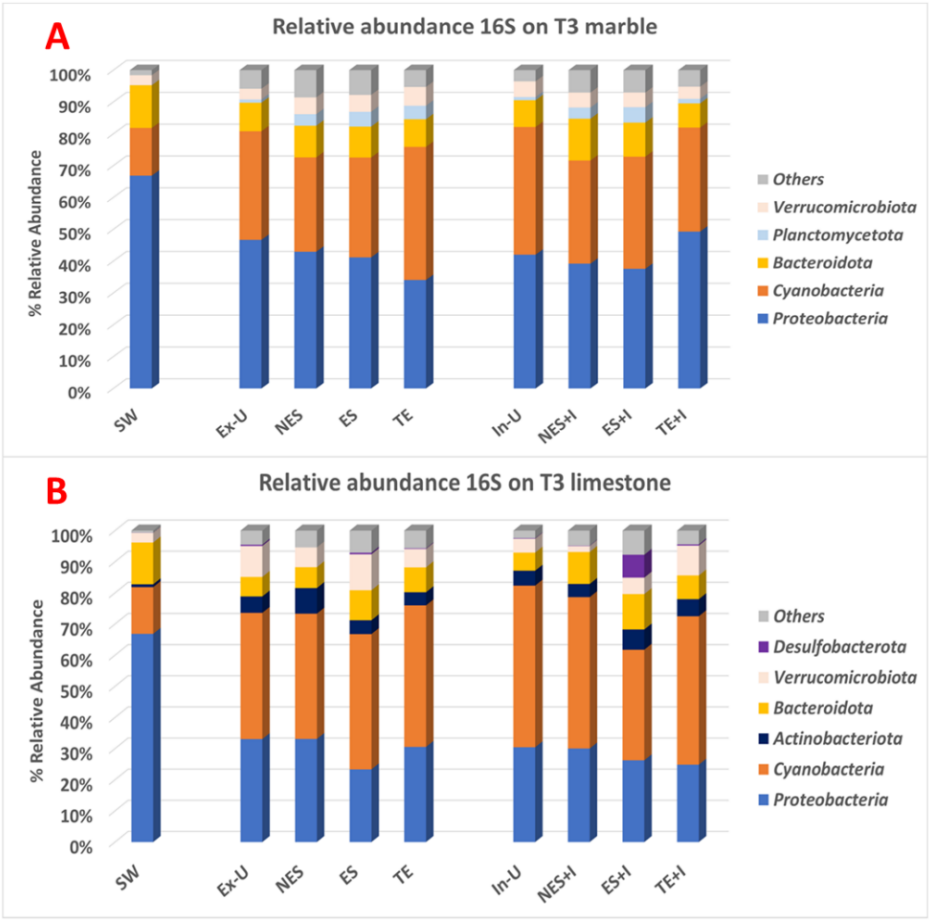

Figure 42. 16S Metabarcoding results obtained from marble **(A.)** and limestone specimens **(B.)** exposed for 12 months *in situ*.

Proteobacteria represented on average 29 % of the relative abundance on the limestone samples (Ex-U= 33.0; NES= 33.1; ES= 23.3; TE= 30.5; In-U= 30.4; NES+I= 30.0; ES+I= 26.2; TE+I= 24.8), 44 % was represented by Cyanobacteria (Ex-U= 40.5; NES= 40.2; ES= 43.5; TE= 45.5; In-U= 51.9; NES+I= 48.6; ES+I= 35.5; TE+I= 47.7) . Only ES+I treatment leads to a slight decrease of Cyanobacteria phylum and increase of Desulfobacterota (In-U= 0.1 %; NES+I= 0.1 %; ES+I= 7.4 %; TE+I= 0.4 %). It is worth noting that Proteobacteria settled more on limestone surfaces than marble ones, vice versa for the phylum Cyanobacteria. Moreover, the relative abundance of the latter was greater on limestone probes placed in the external area of the cage than those placed in the internal part.

The amount of DNA collected from the surfaces treated with bare Nano Estel and combined with IL appeared different from that obtained in other conditions as at T2 time point (Tables 6-8). These surfaces appeared to yield less DNA compared to the other tested conditions.

Table 8. BioSpec-nano quantification of DNA extracted from limestone surfaces exposed for 12 months *in situ* and targeted for sequencing of 16S and 18S regions.

SAMPLING TIME	SURFACE	CND	CONCENTRATION (ng/cm^2)	*se*
T3	**Limestone**	Ex-U	9.09	6.47
		NES	1.51	5.56
		ES	6.66	4.35
		TE	8.20	4.42
		In-U	5.06	4.68
		NES+I	3.71	2.93
		ES+I	8.15	0.95
		TE+I	12.13	5.19

Metabarcoding analysis showed a significant difference between the microbial composition found on specimens exposed in the internal and external sides of the cage at each time point, justifying our choice to place controls in the different areas of the cage. Our results also showed how different treatment and porosity of the surface affect colonization in the marine environment, as different phyla settled on the two lithotypes; together with the many variables that play in the marine biofouling process.

Fouling behavior of treated probes versus untreated ones

The first colonizers of untreated marble surfaces belonged to the phyla Proteobacteria and Cyanobacteria, but also to eukaryotic phyla Ciliophora and Cnidaria. Over the time of exposure, the prokaryotic communities underwent reorganizations and Verrucomicrobiota, Actinobacteria and Plactomycetes dominated the biofilm layer most in contact with the marble surface submerged for 6 months and the eukaryotic phyla such as Cnidaria colonized the outer biofilm layer. Limited data were available for untreated limestone colonizers up to one month, but after 6 months, the community differed from marble, notably lacking Verrucomicrobiota. However, untreated limestone samples were found to be more prone to degradation in the marine environment then marble, in agreement with observations made in previous studies (Casoli et al., 2015). Phylum Bryozoa was found on untreated limestone surfaces but not on marble ones, resulting in degradation by pitting. After 1 year, surfaces of both lithotypes were significantly colonized, covered with an organized biofilm structure characterized by the presence of the phyla Proteobacteria and Cyanobacteria.

Despite their common use for subaerial conservation, Nano Estel, Estel 1000 and TEOS coatings showed not significant antifouling activity underwater (Franzoni et al., 2015; Pozo-Antonio et al., 2019; Masi et al., 2023).

Marble treated with Nano Estel was widely colonized at all time points. The bare consolidant partially interfered with the formation of homogeneous biofilm favoring the formation of microalgal clusters, which decreased significantly with IL addition up to 12 months of exposure. Moreover, the phylum Mollusca colonized untreated marble surfaces exposed in the internal area of the cage for 6 months, but was absent on NES+I specimens. No remarkable differences were observed between NES- and NES+I-treated limestone after 6 months of exposure. Morphological differences in organic coverage were noted between limestone surfaces treated with the bare binder and with the binder plus IL, but these variations were attributable to the spatial placement within the cage. After 12 months the NES and NES+I limestone surfaces appeared widely deteriorated, although the organic coverage appeared less structured on specimens placed in the internal side of the cage.

Evaluation of ES and ES+I-treated surfaces exposed *in situ* revealed differences in biofouling behavior. Marble treated with binder alone deteriorated progressively, with visible grooves appearing after 12 months. ES limestone surfaces followed a similar trend, with microperforations observed after 12 months due to biofouling. In contrast, the ES+I bilayer treatment seemed to protect the stone surfaces. After 1 month and 6 months, colonization occurred on both marble and limestone surfaces, but the resulting damage was less than untreated surfaces. Similar to NES+I, ES+I marble surfaces exhibited small microbial clusters assembled into rarefied biofilm that was significantly lower than ES specimens. The difference resulting from IL treatment was visible after 12 months. Although both lithotypes did not show a thick organic coverage, ES+I marble surfaces appeared less deteriorated, while ES+I limestone showed visible microperforations. Indeed, already after 6 months, ES+I limestone surfaces were 65 % colonized by the phylum Mollusca, which was not present on the ES+I marble specimens.

Stone surfaces with monolayer TE treatment showed a biofouling level comparable to untreated ones, but IL addition partially interfered with the process. After 1 month, marble surfaces treated with TE alone underwent higher microbial colonization and biofilm coverage similar to untreated ones, while TE+I-treated specimens showed a very rarefied coverage. Eukaryotic analysis revealed lower relative abundance of the phylum Mollusca on the TE+I

marble. In fact, after one year, the TE-treated marble surfaces showed microperforations, whereas the TE+I reported only grooves likely caused by biofoulers activity. Interestingly, the monolayer coating appeared more protective for limestone than marble, unlike previous cases. After 6 months, TE treatment appeared to mitigate the formation of biofilm coverage and IL addition inhibited the settlement of biofoulers. After 12 months, organic coverage on TE limestone surfaces was impressive but lower on TE+I surfaces.

CONCLUSIONS

Our results suggest that IL-bilayer treatments effectively mitigate biofouling on marble surfaces. Treatments with Nano-Estel plus IL or Estel 1000 as a consolidant induced microorganisms clustering, which altered and slowed biofilm formation. Moreover, IL reduced macrofoulers recruitment, particularly the phylum Mollusca, thereby limiting damage to submerged stone.

The TE+I monolayer seems to be the best coating for limestone, likely due to its deeper surface penetration. Rather than inhibiting macrofoulers recruitment, it mitigates their interaction with the substrate. Treated surfaces showed less deterioration than those with binder alone and lacked the calcareous encrustations observed on untreated specimens.

Biofouling was also influenced by probes position in the underwater environment, which may have effected exposure to both biotic and abiotic stimuli (e.g., light, current, nutrients and sediment suspension). Our assertions are supported by the fact that all these factors were considered and the key environmental parameters (temperature, salinity, pH and sediment composition) remained throughout the experimental period. Currents and tidal movements, even if inherently uncontrolled, affected the biofouling processes of all stone surfaces uniformly.

FUTURE PERSPECTIVES

The mid-term exploration of antifouling coatings containing *ILs of third generation* represented a crucial step in developing *in situ* protection methods for submerged cultural heritage, aiming to stabilize archaeological sites using more eco-sustainable solutions. Choline, a B-complex vitamin nutrient, in combination with bromide and dodecylbenzenesulfonate (DBS), is generally considered eco-friendly at low concentrations (e Silva et al., 2014). This mixture provided an innovative formulation for the development of multifunctional coatings. Previous *in vitro* studies demonstrated that ionic components with surfactant properties enhanced antimicrobial performance, and current laboratory tests confirmed the compatibility of these formulations with stone substrates when supported by silica-based consolidants.

Nonetheless, the complexity of biodegradation phenomena in the marine environment maked the field study of antifouling activity extremely challenging. The main issue was the unpredictable environmental variations that influence marine biofouling. Notably, several reported studies underline the importance of using spatial control samples, since the biodeterioration processes are affected by the surface position in the submerged environment, even at a very short distance (centimeters). Another major challenge concerns the investigation of the initial stages of biofouling (up to one month). In this context, combined microscopic and molecular techniques proved insufficient. IL-based coatings have clearly shown partial interference with macrofouling, but future formulations should aim to inhibit the earliest phases of biofouling. Avoiding colonization increases the long-term durability of stone coatings, reduce restoration needs, and help maintain public access to UCH. The analysis of untreated stone surfaces could contribute to a deeper knowledge of biofouling processes on submerged inorganic materials. Incorporating dependent and independent culture methods may help to select the microbial strains responsible for biofilm production, which is the beginning of the biofouling process. Knowing their identity and *in situ* activity, may support the development of more efficient antifouling products. The effectiveness of antifouling methods also depends on other factors, such as the mechanism of action, active compound concentration, and exposure time (Cirone et al., 2023). In order to draw reliable conclusions, it is essential to conduct long-term studies of silica-ILs systems in terms of bioavailability and to assess the actual stability and effectiveness of coatings over time. Future research should explore how antimicrobial agents perform in combination with the different consolidants, to tailor treatments according to specific substrates and environmental

conditions. Advancing the conservation of submerged cultural heritage will increasingly rely on targeted interdisciplinary approaches grounded in robust environmental impact assessments, life-cycle analysis, and cost–benefit evaluations. These aspects will be carefully evaluated in order to design IL-based protective coatings for submerged cultural assets.

REFERENCES

Alì, R.H., 2025. Antibiofouling coatings for PMMA photobioreactors (PBRS) and stone-built cultural heritage. University of Messina.

Aloise, P., Ricca, M., La Russa, M.F., Ruffolo, S.A., Belfiore, C.M., Padeletti, G., Crisci, G.M., 2014. Diagnostic analysis of stone materials from underwater excavations: The case study of the Roman archaeological site of Baia (Naples, Italy). Appl Phys A Mater Sci Process 114, 655–662. https://doi.org/10.1007/s00339-013-7890-1

Alvik, R., 2018. Wreck of the dutch merchant ship vrouw maria: Example of protection and management of underwater cultural heritage in baltic waters, in: Competing Values in Archaeological Heritage. Springer International Publishing, pp. 7–24. https://doi.org/10.1007/978-3-319-94102-8_2

Ann, V., Freixa, A., Butturini, A., Romaní, A.M., 2019. Interplay between sediment properties and stream flow conditions influences surface sediment organic matter and microbial biomass in a Mediterranean river. Hydrobiologia 828, 199–212. https://doi.org/10.1007/s10750-018-3812-8

Bekić, L., Ćurković, M., Jelić, A., Jozić, A., Mustaček, M., Perin, T., Pešić, M., 2011. Conservation on of underwater archeological finds manual. Zadar.

Bolyen, E., Rideout, J.R., Dillon, M.R., Bokulich, N.A., Abnet, C.C., Al-Ghalith, G.A., Alexander, H., Alm, E.J., Arumugam, M., Asnicar, F., Bai, Y., Bisanz, J.E., Bittinger, K., Brejnrod, A., Brislawn, C.J., Brown, C.T., Callahan, B.J., Caraballo-Rodríguez, A.M., Chase, J., Cope, E.K., Da Silva, R., Diener, C., Dorrestein, P.C., Douglas, G.M., Durall, D.M., Duvallet, C., Edwardson, C.F., Ernst, M., Estaki, M., Fouquier, J., Gauglitz, J.M., Gibbons, S.M., Gibson, D.L., Gonzalez, A., Gorlick, K., Guo, J., Hillmann, B., Holmes, S., Holste, H., Huttenhower, C., Huttley, G.A., Janssen, S., Jarmusch, A.K., Jiang, L., Kaehler, B.D., Kang, K. Bin, Keefe, C.R., Keim, P., Kelley, S.T., Knights, D., Koester, I., Kosciolek, T., Kreps, J., Langille, M.G.I., Lee, J., Ley, R., Liu, Y.X., Loftfield, E., Lozupone, C., Maher, M., Marotz, C., Martin, B.D., McDonald, D., McIver, L.J., Melnik, A. V., Metcalf, J.L., Morgan, S.C., Morton, J.T., Naimey, A.T., Navas-Molina, J.A., Nothias, L.F., Orchanian, S.B., Pearson, T., Peoples, S.L., Petras, D., Preuss, M.L., Pruesse, E., Rasmussen, L.B., Rivers, A., Robeson, M.S., Rosenthal, P., Segata, N., Shaffer, M., Shiffer, A., Sinha, R., Song, S.J., Spear, J.R., Swafford, A.D., Thompson, L.R., Torres, P.J., Trinh, P., Tripathi, A., Turnbaugh, P.J., Ul-Hasan, S., van der Hooft, J.J.J., Vargas, F., Vázquez-Baeza, Y., Vogtmann, E., von Hippel, M., Walters, W., Wan, Y., Wang, M., Warren, J., Weber, K.C., Williamson, C.H.D., Willis, A.D., Xu, Z.Z., Zaneveld, J.R., Zhang, Y., Zhu, Q., Knight, R., Caporaso, J.G., 2019. Reproducible, interactive, scalable and extensible microbiome data science using QIIME 2. Nat Biotechnol. https://doi.org/10.1038/s41587-019-0209-9

Borkowski, A., Syczewski, M., Czarnecka-Skwarek, A., 2019. Ionic liquids strongly affect the interaction of bacteria with magnesium oxide and silica nanoparticles. RSC Adv 9, 28724–28734. https://doi.org/10.1039/c9ra05110d

Bruno, F., Muzzupappa, M., Barbieri, L., Gallo, A., Ritacco, G., Lagudi, A., La Russa, M.F., Ruffolo, S.A., Crisci, G.M., Ricca, M., Comite, V., Pietraggi, B.D., Di Stefano, G.,

Ageotec, S., Guida, R., 2016. The CoMAS Project: New materials and tools for improving the *in situ* documentation, restoration, and conservation of underwater archaeological remains. Mar Technol Soc J 50, 108–118.

Callahan, B.J., McMurdie, P.J., Rosen, M.J., Han, A.W., Johnson, A.J.A., Holmes, S.P., 2016. DADA2: High-resolution sample inference from Illumina amplicon data. Nat Methods 13, 581–583. https://doi.org/10.1038/nmeth.3869

Callow, M.E., Callow, J.E., 2002. Marine biofouling: a sticky problem. Biologist 49, 10–4.

Cardiano, P., Fazio, E., Lazzara, G., Manickam, S., Milioto, S., Neri, F., Mineo, P.G., Piperno, A., Lo Schiavo, S., 2015. Highly untangled multiwalled carbon nanotube@polyhedral oligomeric silsesquioxane ionic hybrids: Synthesis, characterization and nonlinear optical properties. Carbon N Y 86, 325–337. https://doi.org/10.1016/j.carbon.2015.01.047

Casoli, E., Ricci, S., Belluscio, A., Gravina, M.F., Ardizzone, G., 2015. Settlement and colonization of epi-endobenthic communities on calcareous substrata in an underwater archaeological site. Marine Ecology 36, 1060–1074. https://doi.org/10.1111/maec.12201

Chen, S., Zhou, Y., Chen, Y., Gu, J., 2018. Fastp: An ultra-fast all-in-one FASTQ preprocessor, in: Bioinformatics. Oxford University Press, pp. i884–i890. https://doi.org/10.1093/bioinformatics/bty560

Cirone, M., Figoli, A., Galiano, F., La Russa, M.F., Macchia, A., Mancuso, R., Ricca, M., Rovella, N., Taverniti, M., Ruffolo, S.A., 2023. Innovative methodologies for the conservation of cultural heritage against biodeterioration: A review. Coatings 13. https://doi.org/10.3390/coatings13121986

Crisci, G.M., La Russa, M.F., MacChione, M., Malagodi, M., Palermo, A.M., Ruffolo, S.A., 2010. Study of archaeological underwater finds: Deterioration and conservation. Appl Phys A Mater Sci Process 100, 855–863. https://doi.org/10.1007/s00339-010-5661-9

Davidde, B., 2004. Methods and strategies for the conservation and museum display *in situ* of underwater cultural heritage.

Davidde, B., Ricci, S., Poggi, D., Bartolini, M., 2010. Marine bioerosion of stone artefacts preserved in the Museo archeologico dei Campi Fregrei in the castle of Baia (Naples), Archeologia marittima mediterranea.

De Leo, F., Cardiano, P., De Carlo, G., Lo Schiavo, S., Urzì, C., 2017. Testing the antimicrobial properties of an upcoming "environmental-friendly" family of ionic liquids. J Mol Liq 248, 81–85. https://doi.org/10.1016/j.molliq.2017.10.024

De Leo, F., Marchetta, A., Capillo, G., Germanà, A., Primerano, P., Schiavo, S. Lo, Urzì, C., 2021. Surface active ionic liquids based coatings as subaerial anti-biofilms for stone built cultural heritage. Coatings 11, 1–22. https://doi.org/10.3390/coatings11010026

Dobretsov, S., Abed, R.M.M., Teplitski, M., 2013. Mini-review: Inhibition of biofouling by marine microorganisms. Biofouling 29, 423–441. https://doi.org/10.1080/08927014.2013.776042

Donnelly, B., Sammut, K., Tang, Y., 2022. Materials selection for antifouling systems in marine structures. Molecules 27. https://doi.org/10.3390/molecules27113408

e Silva, F.A., Siopa, F., Figueiredo, B.F.H.T., Gonçalves, A.M.M., Pereira, J.L., Gonçalves, F., Coutinho, J.A.P., Afonso, C.A.M., Ventura, S.P.M., 2014. Sustainable design for environment-friendly mono and dicationic cholinium-based ionic liquids. Ecotoxicol Environ Saf 108, 302–310. https://doi.org/10.1016/j.ecoenv.2014.07.003

Egorova, K.S., Gordeev, E.G., Ananikov, V.P., 2017. Biological activity of ionic liquids and their application in pharmaceutics and medicine. Chem Rev 117, 7132–7189. https://doi.org/10.1021/acs.chemrev.6b00562

Elshaarawy, R.F.M., Tadros, H.R.Z., El-Aal, R.M.A., Mustafa, F.H.A., Soliman, Y.A., Hamed, M.A., 2016. Hybrid molecules comprising 1,2,4-triazole or diaminothiadiazole Schiff-bases and ionic liquid moieties as potent antibacterial and marine antibiofouling nominees. J Environ Chem Eng 4, 2754–2764. https://doi.org/10.1016/j.jece.2016.05.016

Fallah, Z., Zare, E.N., Khan, M.A., Iftekhar, S., Ghomi, M., Sharifi, E., Tajbakhsh, M., Nikfarjam, N., Makvandi, P., Lichtfouse, E., Sillanpaa, M., Varma, R.S., 2021. Ionic liquid-based antimicrobial materials for water treatment, air filtration, food packaging and anticorrosion coatings. Adv Colloid Interface Sci 294. https://doi.org/10.1016/j.cis.2021.102454

Ferraz, R., Branco, L.C., Prudêncio, C., Noronha, J.P., Petrovski, Ž., 2011. Ionic liquids as active pharmaceutical ingredients. ChemMedChem 6, 975–985. https://doi.org/10.1002/cmdc.201100082

Flemming, H.C., Wingender, J., Szewzyk, U., Steinberg, P., Rice, S.A., Kjelleberg, S., 2016. Biofilms: An emergent form of bacterial life. Nat Rev Microbiol 14, 563–575. https://doi.org/10.1038/nrmicro.2016.94

Franzoni, E., Graziani, G., Sassoni, E., Bacilieri, G., Griffa, M., Lura, P., 2015. Solvent-based ethyl silicate for stone consolidation: influence of the application technique on penetration depth, efficacy and pore occlusion. Materials and Structures/Materiaux et Constructions 48, 3503–3515. https://doi.org/10.1617/s11527-014-0417-1

Grenier, R., Nutley, D., Cochran, I., 2006. Underwater cultural heritage at risk: managing natural and human impacts, Special edition. ed. ICOMOS.

Hadfield, M.G., 2011. Biofilms and marine invertebrate larvae: What bacteria produce that larvae use to choose settlement sites. Ann Rev Mar Sci 3, 453–470. https://doi.org/10.1146/annurev-marine-120709-142753

ISO/CIE 11664-4:2019. Colorimetria-Parte 4: Spazio colore L* a* b* CIE 1976. Ente Nazionale Italiano di Unificazione: Milano, Italy.

ISO/CIE 15801:2010. Conservazione dei beni culturali-Metodi di prova-determinazione dell'assorbimento dell'acqua per capillarità. Ente Nazionale Italiano di Unificazione: Milano, Italy.

ISO/CIE 15802:2010. Conservazione dei beni culturali-Metodi di prova-determinazione dell'angolo di contatto statico. Ente Nazionale Italiano di Unificazione: Milano, Italy.

Jordan, A., Gathergood, N., 2015. Biodegradation of ionic liquids-a critical review. Chem Soc Rev 44, 8200–8237. https://doi.org/10.1039/c5cs00444f

La Russa, M.F., Ricca, M., Belfiore, C.M., Ruffolo, S.A., Álvarez, M., Buergo Ballester, D.E., Crisci, G.M., 2015. The contribution of earth sciences to the preservation of underwater archeological stone materials: an analytical approach. International journal of conservation science 6, 335–348.

La Russa, M.F., Ruffolo, S.A., Ricca, M., Ricci, S., Davidde, B., Barca, D., Capristo, V., 2013. A multidisciplinary approach to the study of underwater artefacts: The case of a *Tritone Barbato* marble statue (Grotta Azzurra, Island of Capri, Naples). Periodico di Mineralogia 82, 101–111. https://doi.org/10.2451/2013PM0006

Lam, C., Harder, T., Qian, P.Y., 2003. Induction of larval settlement in the polychaete *Hydroides elegans* by surface-associated settlement cues of marine benthic diatoms. Mar Ecol Prog Ser 263, 83–92.

Liao, M., Shen, K., Ma, K., Chen, Y., Li, P., Gutfreund, P., Hu, X., Petkov, J.T., Lu, J.R., 2025. Unveiling the multifaceted mechanisms of action in nonionic and cationic biocide combinations against Gram-negative bacteria. J Colloid Interface Sci 696. https://doi.org/10.1016/j.jcis.2025.137891

Lo Schiavo, S., De Leo, F., Urzì, C., 2020. Present and future perspectives for biocides and antifouling products for stone-built cultural heritage: Ionic liquids as a challenging alternative. Applied Sciences (Switzerland) 10. https://doi.org/10.3390/APP10186568

López-Arce, P., Zornoza-Indart, A., Gomez-Villalba, L., Pérez-Monserrat, E.M., Alvarez de Buergo, M., Vivar, G., Fort, R., 2013. Archaeological ceramic amphorae from underwater marine environments: Influence of firing temperature on salt crystallization decay. J Eur Ceram Soc 33, 2031–2042. https://doi.org/10.1016/j.jeurceramsoc.2013.03.009

Luci, M., De Leo, F., De Pascale, D., Galasso, C., La Russa, M.F., Lo Schiavo, S., Ricca, M., Ruffolo, S.A., Ruocco, N., Urzì, C., 2023. Surface-active ionic-liquid-based coatings as anti-biofilms for stone: An evaluation of their physical properties. Coatings 13, 1669. https://doi.org/10.3390/coatings13101669

Mallick, H., Rahnavard, A., McIver, L.J., Ma, S., Zhang, Y., Nguyen, L.H., Tickle, T.L., Weingart, G., Ren, B., Schwager, E.H., Chatterjee, S., Thompson, K.N., Wilkinson, J.E., Subramanian, A., Lu, Y., Waldron, L., Paulson, J.N., Franzosa, E.A., Bravo, H.C., Huttenhower, C., 2021. Multivariable association discovery in population-scale meta-omics studies. PLoS Comput Biol 17. https://doi.org/10.1371/journal.pcbi.1009442

Manoudis, P.N., Karapanagiotis, I., Tsakalof, A., Zuburtikudis, I., Kolinkeová, B., Panayiotou, C., 2009. Superhydrophobic films for the protection of outdoor cultural heritage assets. Appl Phys A Mater Sci Process 97, 351–360. https://doi.org/10.1007/s00339-009-5233-z

Masi, G., Dal Pozzo, A., Ugolotti, G., Tugnoli, A., Sassoni, E., 2023. Choosing the consolidant for carbonate substrates: Technical performance and environmental sustainability of selected inorganic and organic products. Constr Build Mater 407. https://doi.org/10.1016/j.conbuildmat.2023.133599

Mesic´, J.M., 2008. A Resource for Sustainable Development: the case of Croatia. WILEY 60, 91–99.

Mieszkin, S., Callow, M.E., Callow, J.A., 2013. Interactions between microbial biofilms and marine fouling algae: A mini review. Biofouling 29, 1097–1113. https://doi.org/10.1080/08927014.2013.828712

Misra, A., Franco Castillo, I., Müller, D.P., González, C., Eyssautier-Chuine, S., Ziegler, A., de la Fuente, J.M., Mitchell, S.G., Streb, C., 2018. Polyoxometalate-Ionic Liquids (POM-ILs) as anticorrosion and antibacterial coatings for natural stones. Angewandte Chemie - International Edition 57, 14926–14931. https://doi.org/10.1002/anie.201809893

Muhammad, M.H., Idris, A.L., Fan, X., Guo, Y., Yu, Y., Jin, X., Qiu, J., Guan, X., Huang, T., 2020. Beyond risk: bacterial biofilms and their regulating approaches. Front Microbiol 11. https://doi.org/10.3389/fmicb.2020.00928

Oksanen J, Simpson G, Blanchet F, Kindt R, Legendre P, Minchin P, O'Hara R, Solymos P, Stevens M, Szoecs E, Wagner H, Barbour M, Bedward M, Bolker B, Borcard D, Carvalho G, Chirico M, De Caceres M, Durand S, Evangelista H, FitzJohn R, Friendly M, Furneaux B, Hannigan G, Hill M, Lahti L, McGlinn D, Ouellette M, Ribeiro Cunha E, Smith T, Stier A, Ter Braak C, Weedon J, 2025. vegan: Community ecology package.

Öniz, H., Khalil, E., Vivar, G., 2024. Protection of underwater cultural heritage. Confédération Mondiale Des Activités Subaquatiques.

Ortmann, N., 2014. Exploring practitioners' attitudes towards *in situ* preservation and storage for underwater cultural heritage.

Pendleton, J.N., Gilmore, B.F., 2015. The antimicrobial potential of ionic liquids: A source of chemical diversity for infection and biofilm control. Int J Antimicrob Agents 46, 131–139. https://doi.org/10.1016/j.ijantimicag.2015.02.016

Persat, A., Nadell, C.D., Kim, M.K., Ingremeau, F., Siryaporn, A., Drescher, K., Wingreen, N.S., Bassler, B.L., Gitai, Z., Stone, H.A., 2015. The mechanical world of bacteria. Cell 161, 988–997. https://doi.org/10.1016/j.cell.2015.05.005

Petkovic, M., Seddon, K.R., Rebelo, L.P.N., Pereira, C.S., 2011. Ionic liquids: A pathway to environmental acceptability. Chem Soc Rev 40, 1383–1403. https://doi.org/10.1039/c004968a

Pournou, A., 2018. Assessing the Long-Term Efficacy of Geotextiles in Preserving Archaeological Wooden Shipwrecks in the Marine Environment. Journal of Maritime Archaeology 13. https://doi.org/10.1007/s11457-017-9176-9

Pozo-Antonio, J.S., Otero, J., Alonso, P., Mas i Barberà, X., 2019. Nanolime- and nanosilica-based consolidants applied on heated granite and limestone: Effectiveness and durability. Constr Build Mater 201, 852–870. https://doi.org/10.1016/j.conbuildmat.2018.12.213

R Core Team, 2024. R: A language and environment for statistical computing. R Foundation for Statistical Computing, Vienna, Austria.

Ricca, M., La Russa, M.F., 2020. Challenges for the protection of underwater cultural heritage (UCH), from waterlogged and weathered stone materials to conservation strategies: An overview. Heritage 3, 402–411. https://doi.org/10.3390/heritage3020024

Ricci, S., Davidde, B., Bartolini, M., Priori, G.F., 2009. Bioerosion of lapideous artefacts found in the underwater archaeological site of Baia (Naples), Archeologia Marittima Mediterranea.

Ricci, S., Pietrini, A.M., Bartolini, M., Perasso, C.S., 2013. Role of the microboring marine organisms in the deterioration of archaeological submerged lapideous artifacts (Baia, Naples, Italy). Int Biodeterior Biodegradation 82, 199–206. https://doi.org/10.1016/j.ibiod.2013.03.016

Ruffolo, S.A., Macchia, A., Russa, M.F. La, Mazza, L., Urzì, C., De Leo, F., Barberio, M., Crisci, G.M., 2013. Marine Antifouling for Underwater Archaeological Sites: TiO_2 and Ag-doped TiO_2. International Journal of Photoenergy 2013. https://doi.org/10.1155/2013/251667

Ruffolo, S.A., Ricca, M., Macchia, A., La Russa, M.F., 2017. Antifouling coatings for underwater archaeological stone materials. Prog Org Coat 104, 64–71. https://doi.org/10.1016/j.porgcoat.2016.12.004

Sacco Perasso, C., Antonelli, F., Calcinai, B., Casoli, E., Gravina, M.F., Ricci, S., 2022. The bioerosion of submerged archeological artifacts in the Mediterranean sea: An overview. Front Mar Sci. https://doi.org/10.3389/fmars.2022.888731

Salaris, V., Brodasca, V., De Santis, H., 2008. Archeologia subacquea. Ananke, Torino.

Schneider, C.A., Rasband, W.S., Eliceiri, K.W., 2012. NIH Image to ImageJ: 25 years of image analysis HHS public access, Nat Methods.

Seddon, K.R., 2003. Ionic liquids: a taste of the future. J. Am. Chem. Soc 2, 948–959.

Seddon, K.R., 1997. Ionic liquids for clean technology. J. Chem. T ech. Biotechnol 68, 351–356.

Semenzin, E., Giubilato, E., Badetti, E., Picone, M., Volpi Ghirardini, A., Hristozov, D., Brunelli, A., Marcomini, A., 2019. Guiding the development of sustainable nano-enabled products for the conservation of works of art: proposal for a framework implementing

the Safe by Design concept. Environmental Science and Pollution Research 26, 26146–26158. https://doi.org/10.1007/s11356-019-05819-2

Skowronek, R.K., Johnson, R.E., Vernon, R.H., Fischer, G.R., Bureuu, F., 1987. The Legare Anchorage shipwreck site-Grave of HMS Fowey, Biscayne National Park, Florida. The international journal of nautical archaeology and underwater exploration 16, 313–324.

Thijs, Maarleveld., 2013. Manual for activities directed at underwater cultural heritage. UNESCO.

UNESCO, 2001. Convention sur la protection du patrimoine cultural subaquatique UNESCO. Paris.

Urzì, C., Albertano, P., 2001. Studying phototrophic and heterotrophic microbial communities on stone monuments. Methods Enzymol 336, 340–355. https://doi.org/10.1016/s0076-6879(01)36600-4

Urzì, C., De Leo, F., 2001. Sampling with adhesive tape strips: an easy and rapid method to monitor microbial colonization on monument surfaces. J Microbiol Methods 44, 1–11. https://doi.org/10.1016/S0167-7012(00)00227-X

Veltri, S., Palermo, A.M., De Filpo, G., Xu, F., 2019. Subsurface treatment of TiO_2 nanoparticles for limestone: Prolonged surface photocatalytic biocidal activities. Build Environ 149, 655–661. https://doi.org/10.1016/j.buildenv.2018.10.038

Wang, C., Bao, W.Y., Gu, Z.Q., Li, Y.F., Liang, X., Ling, Y., Cai, S.L., Shen, H.D., Yang, J.L., 2012. Larval settlement and metamorphosis of the mussel *Mytilus coruscus* in response to natural biofilms. Biofouling 28, 249–256. https://doi.org/10.1080/08927014.2012.671303

Wang, Y., Li, L., 2020. Uncovering the underlying mechanisms governing the solid-like layering of ionic liquids (ILs) on mica. Langmuir 36, 2743–2756. https://doi.org/10.1021/acs.langmuir.9b03865

Wasserscheid, P., Welton, T., 2007. Ionic liquids in synthesis, in: Ionic Liquids in Synthesis. Wiley. https://doi.org/10.1002/9783527621194.fmatter

Welton, T., 1999. Room-temperature ionic liquids. Solvents for synthesis and catalysis. Chem Rev 99, 2071–2083. https://doi.org/10.1021/cr980032t

Wickham, H., 2016. ggplot2: Elegant graphics for data analysis, Use R! Springer International Publishing, Cham. https://doi.org/10.1007/978-3-319-24277-4

Wickham H, François R, Henry L, Müller K, Vaughan D, 2023. dplyr: A grammar of data manipulation.

Xin, B., Hao, J., 2014. Imidazolium-based ionic liquids grafted on solid surfaces. Chem Soc Rev 43, 7171–7187. https://doi.org/10.1039/c4cs00172a

Zhang, J., Kobert, K., Flouri, T., Stamatakis, A., 2014. PEAR: A fast and accurate Illumina Paired-End read mergeR. Bioinformatics 30, 614–620. https://doi.org/10.1093/bioinformatics/btt593

Zheng, B., Wang, L., Liu, L., 2014. Bacterial community structure and its regulating factors in the intertidal sediment along the Liaodong Bay of Bohai Sea, China. Microbiol Res 169, 585–592. https://doi.org/10.1016/j.micres.2013.09.019